Chem Soc Rev

REVIEW ARTICLE

View Article Online
View Journal | View Issue

Synthesis of non-siliceous mesoporous oxides

Dong Gu and Ferdi Schüth*

Cite this: *Chem. Soc. Rev.*, 2014, **43**, 313

Mesoporous non-siliceous oxides have attracted great interest due to their unique properties and potential applications. Since the discovery of mesoporous silicates in 1990s, organic–inorganic assembly processes by using surfactants or block copolymers as soft templates have been considered as a feasible path for creating mesopores in metal oxides. However, the harsh sol–gel conditions and low thermal stabilities have limited the expansion of this method to various metal oxide species. Nanocasting, using ordered mesoporous silica or carbon as a hard template, has provided possibilities for preparing novel mesoporous materials with new structures, compositions and high thermal stabilities. This review concerns the synthesis, composition, and parameter control of mesoporous non-siliceous oxides. Four synthesis routes, *i.e.* soft-templating (surfactants or block copolymers as templates), hard-templating (mesoporous silicas or carbons as sacrificial templates), colloidal crystal templating (3-D ordered colloidal particles as a template), and super lattice routes, are summarized in this review. Mesoporous metal oxides with different compositions have different properties. Non-siliceous mesoporous oxides are comprehensively described, including a discussion of constituting elements, synthesis, and structures. General aspects concerning pore size control, atomic scale crystallinity, and phase control are also reviewed.

Received 10th May 2013

DOI: 10.1039/c3cs60155b

www.rsc.org/csr

1. Introduction

Since the discovery of ordered mesoporous materials in the early 1990s, the interest in this research field has expanded enormously.[1–4] Mesoporous materials possess attractive properties, such as high surface areas, tunable pore sizes and shapes, various structures, and a multitude of compositions, which endow them with potential applications in catalysis, adsorption, sensors, lithium-ion batteries, drug delivery, and nanodevices.[5–21] Among these, silica and aluminosilicates are two of the most frequently studied compositions of the inorganic framework due to their tetra-connected covalent bonds. The geometrical flexibility of the tetrahedral building blocks in silicas and aluminosilicates allows relatively facile synthesis; moreover, these framework compositions are

Max-Planck-Institut für Kohlenforschung, Kaiser-Wilhelm-Platz 1, 45470 Mülheim an der Ruhr, Germany. E-mail: schueth@mpi-muelheim.mpg.de; Fax: +49 208 3062995; Tel: +49 208 3062373

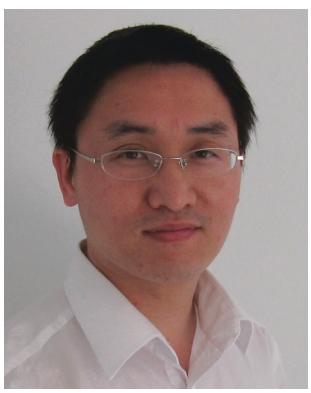

Dong Gu

Dr Dong Gu studied Tourism Management in Department of History at Fudan University (China) in 2001. Then he transferred to Department of Chemistry in 2002 and received a BS degree in 2006. In 2011, he received his PhD degree in inorganic chemistry from Fudan University (supervisor: Prof. Dr Dongyuan Zhao). Since 2011, he has been working in Prof. Dr Ferdi Schüth's group at the Max-Planck-Institute für Kohlenforschung in Mülheim as Post-Doc (Max-Plank fellow and Alexander von Humboldt fellow). He works on the synthesis of mesoporous materials and heterogeneous catalysis.

Ferdi Schüth

Prof. Dr Ferdi Schüth studied Chemistry and Law at Münster, where he received a PhD in chemistry in 1988 and the State Examination in Law in 1989. He was a professor at Frankfurt University before he became director at the Max-Planck-Institute für Kohlenforschung in Mülheim. He has received several awards, among them the Leibniz-Prize of DFG. He is vice president of the German Science Foundation (DFG) and serves on the editorial boards of several international journals. His research interests include catalysis, porous solids, biomass conversion, hydrogen storage, and materials science.

chemically quite stable. Other compositions are susceptible to hydrolysis, redox reactions, or phase transitions, accompanied by thermal breakdown of the structural integrity, which makes it much more difficult to remove the templates and simultaneously retain the ordered mesostructures.[9] Based on mechanistic ideas,[22] non-siliceous mesostructured materials were firstly reported by Huo *et al.*[23] However, for these materials, removal of the templates to produce mesoporous materials failed. Mesoporous non-siliceous materials with open pore structures were first reported by Ying's group in 1995.[24] However, the aqueous solution method analogous to the synthesis of mesoporous silica is not suitable for all non-siliceous materials. Thus, framework compositions were restricted to a very narrow range. With the development of new synthetic strategies, such as evaporation-induced self-assembly (EISA)[25] and nanocasting,[26] a rapid development in the field of non-siliceous materials was started. Yang *et al.*[27–29] used block copolymers as templates, and synthesized a series of mesoporous metal oxides (such as TiO_2, ZrO_2, Nb_2O_5, Al_2O_3, WO_3, HfO_2, and SnO_2) and mixed oxides (such as $SiAlO_{3.5}$, $SiTiO_4$, $ZrTiO_4$, Al_2TiO_5, and ZrW_2O_8). However, these block copolymer derived non-siliceous oxides only have amorphous or semi-crystalline frameworks, since the ordered mesostructures collapse during the thermal crystallization process. Recently, PEO–PPO–PEO (poly(ethylene oxide)–poly(propylene oxide)–poly(ethylene oxide)) type block copolymers have also been used as templates to prepare ordered mesoporous polymers and derived carbons.[30–33] Low molecular weight phenolic resin (resol) has plenty of –OH groups, which can interact with block copolymers through hydrogen bonds. The three-connected benzene ring framework is stable at the temperature of the thermal decomposition of block copolymer templates, leading to highly ordered mesoporous polymers and carbons with open pore structures. Nanocasting, by using pre-formed silicas or carbons as hard templates, makes many non-siliceous materials accessible. Thus, materials that cannot be fabricated using surfactants or block copolymers can be synthesized by the nanocasting method. In addition, materials with crystalline wall structures can be obtained *via* nanocasting pathways. Mesoporous carbon,[26,34] metals,[35] metal oxides,[36,37] phosphates,[38–40] polymers,[41] sulfides,[42,43] and even ceramics[44–46] *etc.* have been prepared by the nanocasting method.

Among the mesoporous non-siliceous materials, mesoporous metal oxides, a big family including most of the metals in the periodic table, are of great interest because of their broad functional properties and their industrial application potential. For example, alumina is widely used as a catalyst support. Titania has potential applications in dye-sensitized solar cells (DSSCs). Cobalt oxide as a CO oxidation catalyst and electrode material for lithium-ion batteries has recently attracted great attention. Several reviews have discussed mesoporous non-siliceous materials, such as carbons,[19] polymers,[47] and non-oxide[20] materials, recently. We thus focus this review only on non-siliceous oxides due to their similarities in synthesis and characterization. Some bi-metalic oxides are also involved. We will also focus on the development in the last ten years, since a comprehensive review covering the state of the art up to 2001 has been authored by one of us.[9]

2. Strategies for the creation of non-siliceous mesoporous oxides

Since the sol–gel chemistry of non-siliceous oxides is much more diverse than that of the siliceous materials, the synthetic strategies for their production need to be versatile. Four pathways leading to mesostructured materials will be discussed in this section. The traditional surfactant/block copolymer based soft-templating method, the mesoporous silica/carbon based hard-templating method (nanocasting), the colloidal crystal templating method, and a new super lattice approach are discussed in the following.

2.1 Soft-templating method

Table 1 summarizes different mesoporous metal oxides synthesized by the soft-templating method. As can be seen, various metal oxides, including those of almost all the light metal elements and lanthanum, are accessible by now, using different surfactants or block copolymers as templates.

The most obvious approach for synthesizing ordered mesoporous metal oxides is the direct adaption of the pathways that have successfully been applied in the synthesis of mesoporous silica. The surfactant or block copolymer based soft-templating method is mostly used in the synthesis of mesoporous silica (Fig. 1). Aqueous solution synthesis and EISA routes are normally adapted for synthesizing mesoporous metal oxides.[20,48] In the solution synthesis route, the key issue is a controllable hydrolysis–condensation behavior of the metal species. A strong interaction between templates and precursors is necessary to form ordered mesostructures and avoid macroscale phase separation. The co-assembly process is driven by weak non-covalent bonds such as hydrogen bonds and electrostatic bonds between the surfactants and the inorganic species. Cooperative assembly between inorganic precursors and surfactants is generally involved simultaneously with the hydrolysis–condensation process, leading to mesostructured composites. After the removal of surfactants, mesoporous metal oxides with open pores can be obtained (Fig. 1). Therefore, the interaction between inorganic species and surfactants is particularly essential for the formation of ordered mesostructures. For the synthesis of mesoporous silica (such as MCM-41), the silicate species are negatively charged under typical conditions, which match the positively charged surfactant through electrostatic interaction. A similar charge interaction or hydrogen-bonding interaction is also necessary for the synthesis of metal oxides. There are four different models, S^+I^-, S^-I^+, $S^+X^-I^+$, and $S^-X^+I^-$, where "S" represents the surfactant, "I" represents the inorganic species, and "X" represents a mediator. Based on this model, the first successful syntheses of mesostructured metal oxides and metal phosphates were reported.[23] Unfortunately, it was not possible to remove the surfactants to obtain porous materials, due to the collapse of the framework. The use of acetylacetone to postpone the precipitation of oxide–alkoxide aggregates led to the synthesis of the first ordered mesoporous non-siliceous oxide Ti-TMS1.[24] The Brunauer–Emmett–Teller (BET) surface area of

Table 1 Non-siliceous mesoporous oxides prepared by soft-templating methods

Product	Template	Structure	Pore size (nm)	V_t [a] ($cm^3\ g^{-1}$)	S_{BET} [b] ($m^2\ g^{-1}$)	Ref.
Al_2O_3	Tergitol, Igepal, Pluronic 64L	Disordered	4.0–8.0	0.21–0.68	425–535	137
	Lauric acid, caproic acid, stearic acid	—	1.9–2.1	0.34–0.58	390–710	197
	SDS	*p6mm*[c] Lamellar	—	—	—	198, 363
	P123	Disordered	14.0	0.61	300	27, 29
	SDS, CTAB, *etc.*	—	0.8–6.0	0.08–0.61	112–810	120
	P84, P123, L64	—	3.7–13	0.39–1.51	249–370	199, 200
	P123	—	10.6	0.59	156–208	201
	P123	*p6mm*	3.9–15.0	0.44–0.80	209–410	166
	KLE	$Fm\bar{3}m$	23	—	—	122
	CTAB, CTACl	Disordered	2.8–9.7	0.40–0.78	296–626	138
	F127	*p6mm*	4.4	0.42	152	56
	P123, F127	*p6mm*	4–7	0.68–0.75	350–460	119, 167
	P123	*p6mm*	8–11	0.3–0.7	200–300	168
	F127 and PMMA	—	—	0.36–0.68	118–145	323
	CTAB and citric acid	Disordered	3.5–23	0.24–0.59	85–398	139, 140
	P123	*p6mm*	4.0–10.5	0.06–0.74	26–583	169
	F127	$Im\bar{3}m$	—	—	—	187
	PS-*b*-PEO	—	35–80	—	—	364
Bi_2O_3	KLE	Cubic	14–16	25–30%[d]	140	123
CaO	P123/CTAB/PEG	Disordered	3.3–5.0	0.19–0.29	110–257	322
CeO_2	P123	Disordered	3.5	—	86–150	313, 365
Co_3O_4	P123	*p6mm*	10.0	2.07	367	296
Cr_2O_3	F127	$Im\bar{3}m$	7.9	—	78–212	188
Cu_2O	Brij	*p6mm*[c]	—	—	—	303
	P123	Disordered	7.4	0.11	48	304
Dy_2O_3	SDS	*p6mm*	2.5–3.0	—	253	117
Er_2O_3	SDS	*p6mm*	2.5–3.0	—	280	117
	Hexadecylamine	$Ia\bar{3}d$	2.2	—	60	118
Eu_2O_3	KLE	$Im\bar{3}m$	10–13	45–49%[d]	—	124
	F127	Disordered	17.1	0.13	32	366
Fe_2O_3	CTAB	Disordered	3.9, 7.5	—	94–274	141
	Alkyl amines Alkyl carboxylates	Disordered[c]	—	—	—	142
	Decylamine	*p6mm*	—	—	340	170
		$Fm\bar{3}m$	—	—	610	
	PIB-*b*-PEO, KLE	$Im\bar{3}m$	8	—	150	125
	KLE	Distorted cubic	14–15	29%[d]	190[e]	276
Ga_2O_3	SDS	Disordered	—	—	233	143
	CTAB, P123, F127	Disordered	2.0–12.2	0.11–0.70	70–360	343, 344
Gd_2O_3	SDS	*p6mm*	2.5–3.0	—	287	117
	Hexadecylamine	$Ia\bar{3}d$	2.1	—	98	118
HfO_2	CTAB	Disordered	1.1	—	204	144
	P123	—	7.0	0.52	105	27, 29
	KLE	$Im\bar{3}m$	5.5	0.31	130–160	126
Ho_2O_3	SDS	*p6mm*	2.5–3.0	—	316	117
	CTAB	Lamellar	—	—	—	350
IrO_2	PEO–PB–PEO	—	16	—	83–248	367
La_2O_3	Hexadecylamine	$Ia\bar{3}d$	3.2	—	240	118
	SDS	*p6mm*, lamellar[c]	—	—	—	368
Lu_2O_3	SDS	*p6mm*	2.5–3.0	—	257	117
MgO	F127 and PMMA	Disordered	—	0.36–0.49	125–243	323
	PEO–PB–PEO	Disordered	—	—	—	324
MnO_2	Alkyl amines, alkyl carboxylates	Disordered[c]	—	—	—	142
γ-MnO_2	CTAB	Disordered	3.6	—	316	270
Mn_2O_3	CTAB	*p6mm*	3.0	—	170	171
Mn_3O_4		Cubic	—	—	46	
MoO_2	Bis(trimethylsilyl) dodecylamine	*p6mm*, lamellar[c]	—	—	—	255
MoO_x	PEO	Primitive cubic	2.4	—	212	193
	Gemini	Lamellar	1.8–2.1	—	116	260, 261
α-MoO_3	KLE	$Fm\bar{3}m$	13	30%[d]	200	127
Nb_2O_5	Amine *etc.*	*p6mm*, $P6_3/mmc$, lamellar	2.2–3.9	—	380–713	172, 238, 239
	Hexylamine	*p6mm*	<2.0	—	120–250	173
	P123	*p6mm*	5.0	0.50	196	27, 29
	P85	$P6_3/mmc$	5.0	—	201–220	190
	P123	*p6mm*	2.0–6.0	0.06–0.21	105–190	174, 175
	F127	*p6mm*	4.0	0.36	78	56
	P123	Disordered	4.3–7.5	0.16–0.18	84–164	240
	PI-*b*-PEO	*p6mm*	34.5	—	54	133

Table 1 (*continued*)

Product	Template	Structure	Pore size (nm)	V_t [a] ($cm^3\ g^{-1}$)	S_{BET} [b] ($m^2\ g^{-1}$)	Ref.
	KLE	$Im\bar{3}m$	13–15	28–31%[d]	150	128
	P123	$Ia\bar{3}d$	5.0	0.29	183	241
Nd_2O_3	Hexadecylamine	$Ia\bar{3}d$	2.4	—	133	118
NiO	Brij56/78	*p6mm*[c]	—	—	—	369
	SDS	*p6mm*	4.0–7.0	0.16–0.46	72–279	176
	SDS	Disordered	3.6–7.4	0.39–0.60	217–478	145
	SDS, P123, F127, PEG	*p6mm*, lamellar[c]	—	—	—	370
	Brij56	*p6mm*	2.5	—	—	177
Pr_2O_3	Hexadecylamine	$Ia\bar{3}d$	2.3	—	125	118
RuO_2	P123	Disordered	—	—	—	298
	PS–PEO	Disordered	25–35	—	—	135
	P123	Disordered	10.2–13.5	—	87	371
	SDS + CTAB	Lamellar	0.92	—	—	372
	Brij 56	*p6mm*	—	—	100	373
Sm_2O_3	Hexadecylamine	$Ia\bar{3}d$	2.4	—	122	118
	F127	Disordered	11.5	0.23	28	366
SnO_2	AOT	*p6mm*[c]	3.0	—	—	178
	Tetradecylamine	Disordered	1.4–4.3	0.15	99–314	146
	SDS	Disordered[c]	—	—	—	374
	P123	*p6mm*	6.8	0.52	180	27, 29
	Tetradecylamine	Disordered	—	—	107	375
	CTAB	Disordered	—	—	143	
	C_{16}PyCl	*p6mm*	1.6–3.6	—	98–374	179, 180
	Brij	*p6mm*[c]	—	—	—	376
	CTAB	Disordered	2.9–6.0	0.20–0.27	166–220	377
	PB–PEO	Cubic	18–20	0.28	66	113
	KLE	$Im\bar{3}m$	6.7–14.2	45.5%[d]	130[e]	129
	CTAB	Disordered	3.7, 7.8	—	94	352
Ta_2O_5	Octadecylamine	*p6mm*	2.2–3.4	—	436–510	181, 182
	P123	*p6mm*	3.5	0.50	165	27, 29
	F127	*p6mm*	4.5	0.45	98	56
	KLE	$Im\bar{3}m$	14	—	—	128
Tb_2O_3	SDS	*p6mm*	2.5–3.0	—	348	117
TiO_2	Tetradecylphosphate	*p6mm*	3.2	—	100–200	24
	$C_{12}EO_5$	Disordered	4.5	—	350	209
	Amine	*p6mm*[c]	2.9–3.2	—	—	178
	P123	*p6mm*	6.5	0.46	205	27, 29
	$EO_{75}BO_{45}$	$Im\bar{3}m$				
	Amine	Wormhole-like	1.5	0.53	79–853	147
	P123	—	2.0–8.0	0.13–0.37	150–242	378
	CTAB	*p6mm*	3.5	—	606	379
	P123	*p6mm*	—	—	—	380
	P123, B50-6600, Brij 97, CTAB, F108	*p6mm*	1.9–5.5	0.14–0.36	139–275	201
	P123	Disordered	6.0–9.2	0.24–0.30	112–192	381
	P123	Lamellar, *p6mm*, $Im\bar{3}m$	—	—	—	211
	Amine	Disordered	2.3–5.9	0.07–0.65	154–1256	382
	CTAB	*p6mm*	1.9–2.5	0.16–0.19	266–370	52
	P123, F127, Brij	*p6mm*, $Im\bar{3}m$	7.0	40%[d]	100–150	54, 55
	P123	*p6mm*	6.3–7.3	—	172–206	215
	KLE	$Im\bar{3}m$	10	—	—	130
	P123	Cubic	5.5	—	175	383
	CTAB	*p6mm*	—	—	262	217, 218
	F127	*p6mm*	5.0	0.48	191	56
	P123, 1-butanol	$R\bar{3}m$	20	45%[d]	—	192
	Tween 80	Disordered	4.0–6.9	46–69%[d]	147–159	216
	Dodecyl sulfate	*p6mm*	2.7	—	128	384
	F127	—	—	—	—	385
	P123	$P6_3/mmc$	—	—	58	191
	P123	*p6mm*	6.7	—	200–208	183
	P123	*p6mm*	5.7–7.6	0.26–0.38	171–271	184
	F127, polymer	*p6mm*	3.0–11.4	0.16–0.26	191–465	185, 186
	F127	$Im\bar{3}m$	—	—	—	386, 387
	PI-*b*-PEO	*p6mm*	22.9	—	89	133, 134
	P123	$P6_3/mmc$	—	74–137[f]	322–595[e]	388
	P123	*p6mm*	4.6–6.5	0.23	180–202	160
	PS-*b*-PEO	Primitive cubic	15.3–16.1	0.18–0.27	80–112	136
	F127	*p6mm*	3–5	0.14	44–113	389
	PEO–PB–PEO	$Im\bar{3}m$	7.6–21.1	—	85–328	189
	F127	—	5.3–6.4	0.25–0.36	143–232	390

Table 1 (*continued*)

Product	Template	Structure	Pore size (nm)	V_t [a] ($cm^3\ g^{-1}$)	S_{BET} [b] ($m^2\ g^{-1}$)	Ref.
	P123	*p6mm*	9.8	0.52	370	391
	PI–PS–PEO	Gyroid-like	18.0–21.0	—	—	392
Tm_2O_3	SDS	*p6mm*	2.5–3.0	—	335	117
V_2O_5	CTACl	Lamellar, *p6mm*	—	—	60	235, 236
	Dodecylamine	Lamellar, *p6mm*[c]	—	—	—	237
	P123	Disordered	3–4	0.56	—	393
	Brij	C_2m[c]	—	—	—	51
	CTAB, HDA	—	4.7	0.21	218	234
WO_3	Cationic surfactant	*p6mm*, lamellar[c]	—	—	—	23, 196
	P123	*p6mm*	5.0	0.48	125	27, 29
	P123	Disordered	5.0–10.6	0.46–0.55	45–155	394
	SDS	Wormhole-like, lamellar	1.5–2.5	—	—	148
	KLE	$Im\bar{3}m$	6	—	150–180	131
	Gemini	Disordered	3.7	0.14	145	395
Y_2O_3	F127	Disordered	6–8	—	19–49	396
	KLE	Disordered	8–14	27–32%[d]	—	132
Yb_2O_3	SDS	*p6mm*	2.5–3.0	—	283	117
	Hexadecylamine	$Ia\bar{3}d$	2.5, 5.8	—	55	118
ZnO	Brij	*p6mm*	—	—	—	303
	Eosin	Disordered	>8.0	60%[d]	140[g]	305
	L_{16}	Disordered	2.6	0.24	456	306
ZrO_2	Alkyltrimethylammonium bromide	*p6mm*	1.9–2.5	0.12–0.26	230–540	227, 228
	Amine	Disordered	—	0.24–0.60	164–360	229, 230
	Carboxylate amphiphiles, dodecyl sulfate, alkylsulfonate, amine, phosphate compounds	Lamellar, disordered	1.5–4.0	0.21–0.33	200–400	149
	P123	*p6mm*	5.8	0.43	150	27, 29
	$N(C_n)_4Br$, $N(CH_3)_3C_nBr$	—	>2.0	—	2–359	397
	CTAB	*p6mm*	2.2	—	202	226
	P123	—	4.2	0.21	141–163	201
	CTAB	Disordered	1–2	1.01	903	398
	CTMA	*p6mm*	1.1–3.0	0.01–0.15	15–239	232
	F127	*p6mm*	4.0	0.36	78	56
	F127	*p6mm*	6.2	0.06	56	399
	F127	Distorted *p6mm*	10.5	—	—	400

[a] V_t: total pore volume. [b] S_{BET}: surface area calculated from the application of the BET equation to the nitrogen isotherm. [c] Do not remove the template. [d] Porosity. [e] $m^2\ cm^{-3}$. [f] $cm^3\ cm^{-3}$. [g] $cm^2\ cm^{-2}$.

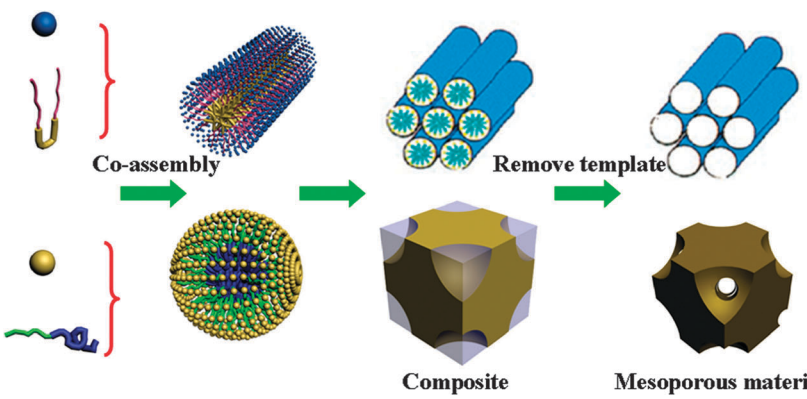

Fig. 1 Schematic representation of the soft-templating pathway leading to mesoporous non-siliceous materials. Different kinds of templates co-assembling with inorganic species can form different mesostructures.

mesoporous Ti-TMS1 reached 200 $m^2\ g^{-1}$ after removing the template by calcination at 350 °C.

In the EISA route, the use of non-aqueous solvents strongly slows down the hydrolysis and condensation rate of metal species, which is highly beneficial for the formation of ordered mesostructures.[25,49] Following this strategy, inorganic precursors with low polymerization degrees are dissolved in volatile polar solvents with weak polarity, which can improve the assembly at the inorganic–organic interface. With the evaporation of the solvent, the surfactants become highly concentrated and form a liquid-crystal phase in the presence of inorganic species, leading to ordered composite mesostructures. The inorganic frameworks

can be further solidified by post treatment and the surfactants can be easily removed by calcination. Yang *et al.* first used an amphiphilic block copolymer as a soft template to prepare mesoporous metal oxides through the EISA process. The relatively weak coordination interaction at the inorganic/organic interface promotes the cooperative assembly of inorganic–polymer composite mesostructures, yielding mesostructured, thermally stable materials. If hydrolysis and condensation rates of metal precursors are too fast, dense inorganic networks lead to poorly ordered mesostructured materials. One solution is the addition of complexing molecules or acids as stabilizing agents. Sanchez and coworkers have published a series of studies on the controllable synthesis of high-quality mesoporous metal oxides with long-range order.[49–55] Some years ago, Fan and coworkers[56] developed an acetic acid assisted sol–gel system (AcHE), which could be broadly applicable for the preparation of thermally stable ordered multicomponent mesoporous metal oxides.

Based on a similar approach as for EISA, ''spray-drying'' has been developed to synthesize mesoporous materials with various structures and compositions.[57,58] Spray-drying methods only involve a limited number of preparation steps that are compatible with on-line continuous production. The resulting materials are obtained in the form of powders with particle sizes that can be tuned between 100 nm and 20 μm through an appropriate choice of the set-up. By combining the sol–gel growth of inorganic networks with the self-assembled surfactant mesophases and aerosol processing, several kinds of mesoporous metal oxides (such as TiO_2,[59,60] ZrO_2,[60] Al_2O_3,[60–62] RuO_2,[63] Nb_2O_5,[63] *etc.*) can be obtained.

2.2 Hard-templating method (nanocasting)

Since many mesostructured materials cannot be obtained by soft-templating processes, the possibility of using ordered mesoporous silicas as molds has been realized.[9] With this nanocasting method, exciting new possibilities for the preparation of novel mesostructured materials became available.[64] The nanocasting method was originally developed for templating from porous Al_2O_3 membranes.[65] Metal, metal oxide and metal sulfide nanostructures can be prepared by introducing precursors into the pore channels through electrodeposition or chemical vapor deposition (CVD) techniques, followed by etching of the templates.[66] Mesoporous materials, especially mesoporous silicas, have highly ordered nanoscale structures and very uniform pore size distributions, and are therefore ideal hard templates for the synthesis of mesostructured materials. Generally, there are several advantages associated with mesoporous materials obtained by hard templating: (a) the smallest features of the replica nanowire arrays or nanostructures have low diameters, usually less than 10 nm; (b) the replica materials usually have three-dimensional (3-D) connected frameworks; alternatively, nanowire arrays are connected by small pillars formed from the micro- or mesochannels inside the pore walls of the templates, leading to the high surface areas and uniform pore size distributions of these materials; (c) the mesostructures can be adjusted by choosing different templates; (d) nanostructured materials with crystalline or even single crystal frameworks can be obtained by high temperature treatment while still protected by the template; and (e) this synthesis strategy circumvents the necessity to control the hydrolysis–condensation process of the inorganic species and the cooperative assembly of surfactants and inorganic species, making it suitable for a wide variety of materials.

The nanocasting process can be represented as shown in Fig. 2, typically including four steps: (1) template preparation; (2) impregnating a guest precursor into the pore system of the template; (3) heating or other treatment to transform the precursor into the target product; and (4) template removal.

Firstly, a suitable template is important. Different mesostructured templates can be replicated into different mesostructured target materials after nanocasting: a unidimensional cylindrical pore system results in nanowire/tube arrays, bicontinuous pore systems result in bicontinuous or lower symmetry replica, and spherical pores result in nanosphere arrays.[16,64,67] Depending on the connectivity of the pores, especially in the case of unidimensional cylinders or spheres, disordered materials or organized 3-D replicas result. In fortunate cases, also the morphologies of the templates can be copied.[68–70] It is worth mentioning that the replica material can also be further used as a hard template for yet another framework.[71–77] Secondly, the choice of a suitable precursor is crucial. For the wet impregnation method, the precursor should be liquid, either as a melt or dissolved in a solvent. In this form, the precursor can easily be filled into the pore systems by capillary force. The precursor also should be inert to the template, so that no reaction can occur during the filling or the transfer process. Thirdly, a suitable method for infiltrating guest precursors into the pores is needed. The most often used method is evaporation induced capillary condensation. During the evaporation process, the solvent outside of the template particles evaporates more rapidly, leading to introduction of the remaining liquid into the pores by capillary force.[37,78,79] Many

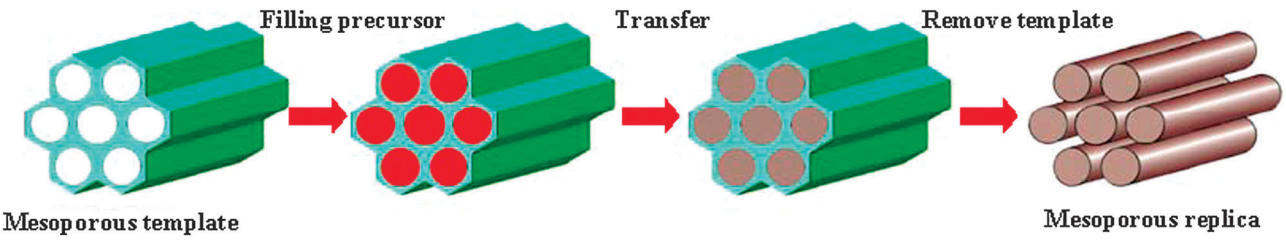

Fig. 2 Schematic representation of the hard-templating (nanocasting) pathway leading to mesoporous non-siliceous materials.

other methods can also be used, such as the surface function method,[36] a two solvent method,[80] melt methods,[81,82] or an organic solvent reflux method.[83] The fourth step is the transformation of the precursor inside the pore system of the template into the target materials. Materials templated from mesoporous silica can be directly calcined in air. For carbon templated or oxygen sensitive materials, an inert atmosphere is needed during the thermal treatment process.[77,84,85] Recently, Sun *et al.*[86] found that the size and shape of the container body in conjunction with the accessibility of the container opening can be used to control the escape rate of water and other gas phase by-products of the calcination process, which in turn affects the nanocrystal growth of the materials inside the mesopore space of the template. The final step is template removal. The silica framework can be dissolved either by NaOH solution or HF solution. Which method should be used depends on the stability of the target material under the leaching conditions. Some materials are stable in both conditions. Carbon templates are most easily removed by calcination in air.[87]

Table 2 summarizes different non-siliceous mesoporous oxides synthesized by the hard-templating method. The preparation of metal oxides by a nanocasting strategy makes it possible to obtain mesostructured materials, which are normally difficult to produce by using soft-templating techniques. This constitutes an additional advantage of the hard-templating over the soft-templating routes.[67]

The first nanostructured metal oxide synthesized by nanocasting is Cr_2O_3 with SBA-15 as a template.[36] The material obtained is a reversed 2-D hexagonal structure formed by nanorod arrays with a diameter of 8 nm. The BET surface area of this kind of Cr_2O_3 material is 58 $m^2 g^{-1}$ (Table 2). Considering the high density and low microporosity of Cr_2O_3, this number is quite high. It is believed that the hydrophilic surface properties caused by the silanol groups favor the impregnation process. The Zhao group[88,89] employed a microwave digestion method to remove organic templates without affecting the surface silanol groups of mesoporous silica. By using such microwave digested silicas as templates, the group has synthesized a series of ordered mesoporous metal oxides.[37,79] Following this procedure, nanowire/rod arrays of Cr_2O_3, Mn_2O_3, Fe_2O_3, Co_3O_4, NiO, In_2O_3 and CeO_2 can be obtained. Using cubic mesoporous silica as templates, nanosphere arrays and bicontinuous mesoporous metal oxides can also be obtained.[37,79] Other mesoporous metal oxides, such as Al_2O_3, CoO, CuO, Fe_3O_4, Ga_2O_3, MgO, MnO_2, RuO_2, SnO_2, TiO_2, ZnO, and ZrO_2, were also successfully prepared by the nanocasting method with mesoporous silica or carbon as hard templates. All these results with the corresponding references are summarized in Table 2. More recently, the Schüth group[90] used a post-synthetic solid–solid reaction method to transfer the ordered mesoporous Co_3O_4 nanocasted from KIT-6 to a Co_3O_4–$CoFe_2O_4$ nanocomposite (Fig. 3). This nanocomposite material behaves as an exchange coupled system with a cooperative magnetic switching.

2.3 Colloidal crystal templating

Colloidal crystal templating is normally used to fabricate 3-D macroporous networks with pore diameters of a few hundred nanometers.[91,92] Polystyrene (PS), poly-(methyl methacrylate) (PMMA), and silica spheres are used as templates to fabricate 3-D macroporous materials with various compositions, including polymers, carbons, metal oxides, and metal sulfides. The general concept of colloidal crystal templating is similar to the nanocasting method: form a colloidal crystal of close-packed and uniformly sized spheres, fill the interstitial spaces with a fluid precursor capable of solidification, transform the precursor into the target product, and remove the template to obtain a porous inverse replica, as schematically illustrated in Fig. 4.[93–95] The colloidal crystal templating approach is versatile and can be applied to different kinds of precursors to produce various metal oxides, for instance, of Ti,[96–102] Zr,[98] Al,[96,98] W, Fe, Sb[98,103] and many other elements. Polymerization of organic precursors within a silica colloidal crystal template results in mesoporous polymers.[104] The pore size of mesoporous polymers (poly-(divinylbenzene) (PDVB), poly-(ethyleneglycol dimethacrylate) (PEDMA)) can be varied continuously between 35 and 15 nm because the polymer shrinks when the 35 nm silica template is removed. Jaroniec and coworkers[105] used mesophase pitch as a carbon precursor and colloidal silica particles as a template to synthesize mesoporous carbon materials with pore sizes between 13 and 24 nm.

The combination of surfactant derived soft-templating and colloidal crystal templating methods offers an efficient way for the construction of ordered and interconnected mesoporous–macroporous architectures.[28,106,107] The colloids usually have particle sizes of at least a few tens of nanometers and a high level of monodispersion, allowing them to aggregate in a regular fashion. This allows infiltration of the inorganic precursor and surfactant composite solution in the space between the colloidal spheres. After solidification of the inorganic framework and removal of both the surfactant and colloidal templates, 3-D ordered meso-/macroporous materials can be obtained. The macropores are connected by the mesopores in the walls, facilitating diffusion of guest species within the pore system. Hierarchical mesoporous metal oxides have been synthesized by such a dual-templating method, including titania,[28] niobia,[28] and silica–alumina.[108] Infiltration of the polymeric scaffold is also possible using plain porous PS films as templates, allowing formation of TiO_2-based pillared structures with hierarchical mesoporosity[109] or gyroidal-like porous titania[110] or vanadium oxides.[111]

2.4 Super lattices

Soft-templating methods are best suitable for the synthesis of mesoporous metal oxides with an amorphous or a half-crystalline framework,[27] while the synthesis of fully crystallized metal oxides is very difficult following this pathway. This is mainly due to the fact that the mesostructures collapse during the annealing step required for the crystallization. One possibility for solving this problem is the use of pre-formed and fully crystallized nanoparticles as building blocks instead of molecular precursors. The experimental procedure is closely related to the EISA process normally used in the soft-templating method. The difference is the use of crystalline colloidal particles instead of inorganic precursors. Surfactants or block copolymers are used as the porogen (Fig. 5). Such a method is also similar to the process for preparing nanoparticle super lattices, so it can be termed the "super lattice

Table 2 Non-siliceous mesoporous oxides prepared by hard-templating methods

Product	Template	Structure	Pore size (nm)	V_t [a] ($cm^3\ g^{-1}$)	S_{BET} [b] ($m^2\ g^{-1}$)	Ref.
Al_2O_3	Carbon aerogels	Disordered	7.7–17.9	0.22–1.55	275–335	202
	CMK-3	*p6mm*	4.6–6.1	0.46–0.55	257–396	203
	FDU-15	*p6mm*	4.1–5.6	0.16–0.61	141–357	87
	CMK-8	*Ia*$\bar{3}$*d*	6.9	0.81	303	401
CeO_2	SBA-15, KIT-6	*p6mm*, *Ia*$\bar{3}$*d*	3.5	0.24	198	317
	KIT-6	*Ia*$\bar{3}$*d*	6.7	0.18	112	318
	CMK-3	*p6mm*	5, 35	0.42	148	319
	KIT-6	*Ia*$\bar{3}$*d*	3.2	—	152	292
	SBA-15	*p6mm*	3.3–3.8	0.23–0.37	101–164	289
	SBA-16	*Im*$\bar{3}$*m*	—	—	—	82
	FDU-12	*Fm*$\bar{3}$*m*	—	—	—	
Co_3O_4	MWD-SBA-15	*p6mm*	3.4	0.37	82	37
	MWD-SBA-16	*Im*$\bar{3}$*m*	6.5	0.33	92	
	FDU-5	*Ia*$\bar{3}$*d*, $I4_132$	—	>0.15	>70	79
	Vinylsilica	*Ia*$\bar{3}$*d*	3.8	0.22	122	153
	SBA-15	*p6mm*	—	—	—	286
	KIT-6	*Ia*$\bar{3}$*d*	4, 9	0.17	92	
	SBA-15	*p6mm*	3.4–5.1	0.14–0.22	101–122	155, 156, 287
	KIT-6	*Ia*$\bar{3}$*d*/$I4_132$	4–10	0.1–0.47	83–152	
	SBA-16	*Im*$\bar{3}$*m*	—	—	122–298	82
	FDU-12	*Fm*$\bar{3}$*m*	—	—	151–450	
	SBA-15	*p6mm*	4	—	90	288
	KIT-6	*Ia*$\bar{3}$*d*	4	—	130	
	SBA-15	*p6mm*	3.6–3.8	0.14–0.15	76–94	289
	LP-FDU-12	*Fm*$\bar{3}$*m*	8.1–8.3	0.09–0.22	30–53	290
CoO	KIT-6	*Ia*$\bar{3}$*d*	4	0.14	55	282, 291
Cr_2O_3	SBA-15	*p6mm*	3.4	0.14	58	36
	MWD-SBA-15	*p6mm*	3.6	0.34	65	37
	KIT-6	*Ia*$\bar{3}$*d*	3.1, 12.3	0.61	86	80
	SBA-15	*p6mm*	—	—	—	247, 286
	KIT-6	*Ia*$\bar{3}$*d*	0–13	0.46	74	
	KIT-6	*Ia*$\bar{3}$*d*	3.1–12.1	0.13–0.22	48–82	402
	KIT-6	*Ia*$\bar{3}$*d*	5.6–7.5	0.10–0.19	73–106	249
	SBA-15	*p6mm*	3.3	0.23	88	248
	KIT-6	*Ia*$\bar{3}$*d*	2.8	0.25	93	
	KIT-6	*Ia*$\bar{3}$*d*	2.5/11.0	0.18–0.24	72–92	246
CuO	CMK-3	*p6mm*	5.5	0.22	149	84
α-Fe_2O_3	MWD-SBA-15	*p6mm*	4.0	0.43	137	37
	KIT-6	*Ia*$\bar{3}$*d*	3.9	—	139	78
	KIT-6	*Ia*$\bar{3}$*d*	4	—	108	277
γ-Fe_2O_3	KIT-6	*Ia*$\bar{3}$*d*	3.6	—	86	278
	SBA-15	*p6mm*[c]	—	—	—	279
	KIT-6	*Ia*$\bar{3}$*d*	4	—	88	277
Fe_3O_4	SBA-15	*p6mm*[c]	—	—	—	280
	KIT-6	*Ia*$\bar{3}$*d*	—	—	—	278
Ferrihydrite	SBA-15	*p6mm*	5.2	0.39	228	281
	KIT-6	*Ia*$\bar{3}$*d*	5.1	0.54	222	
Ga_2O_3	CMK-3	*p6mm*	6.3	0.54	307	403
In_2O_3	MWD-SBA-15	*p6mm*	3.5	0.36	70	37
	MWD-SBA-16	*Im*$\bar{3}$*m*	6.1	0.34	123	
	SBA-15	*p6mm*	2.6	0.43	153	161, 345
	KIT-6	*Ia*$\bar{3}$*d*	2.7	0.45	170	
	FDU-5	*Ia*$\bar{3}$*d*, $I4_132$	—	>0.15	>70	79
	SBA-16	*Im*$\bar{3}$*m*	—	—	—	82
	FDU-12	*Fm*$\bar{3}$*m*	—	—	—	
	CMK-3	*p6mm*	7.0	0.17	39	348
	SBA-15	*p6mm*	9.2–9.6	0.14–0.26	52–87	346
	KIT-6	*Ia*$\bar{3}$*d*	7.8–9.1	0.13–0.27	80–90	
	SBA-15	*p6mm*	2.5–6.5	0.21–0.42	53–126	347
MgO	Carbon	Disordered	7.2–17.8	0.42–0.73	86–154	325
	CMK-3	*p6mm*	5.6–7.0	0.51–0.52	208–306	77, 85
	CMK-3	*p6mm*	6.4–9.5	0.18–0.49	111–256	326
Mn_xO_y	MWD-SBA-15	*p6mm*	3.4	0.39	103	37
β-MnO_2	SBA-15	*p6mm*[c]	—	—	—	404
	KIT-6	*Ia*$\bar{3}$*d*	4.9, 18.2	0.38	84	271
	KIT-6	*Ia*$\bar{3}$*d*	3.3–3.7	0.23–0.48	87–133	272, 273
	SBA-15	*p6mm*	3.8	0.38	142	274
	KIT-6	*Ia*$\bar{3}$*d*	3.6, 30	0.55	87	275
Mn_2O_3	KIT-6	*Ia*$\bar{3}$*d*	3.6	—	139	405
Mn_3O_4	KIT-6	*Ia*$\bar{3}$*d*	3.8	—	100	405

Table 2 (*continued*)

Product	Template	Structure	Pore size (nm)	V_t [a] ($cm^3\ g^{-1}$)	S_{BET} [b] ($m^2\ g^{-1}$)	Ref.
NiO	MWD-SBA-15	*p6mm*	3.5	0.38	56	37
	SBA-15	*p6mm*	4.0	—	47	297
	SBA-16	$Im\bar{3}m$	—	—	—	82
	FDU-12	$Fm\bar{3}m$	—	—	—	
	KIT-6	$Ia\bar{3}d$	3.1–33	—	82–109	154
RuO_2	KIT-6	$I4_132$	3, 15–20	0.42	131	299
SnO_2	SBA-15	*p6mm*	—	—	160	353
	KIT-6	$Ia\bar{3}d$	3.8	0.34	80	
TiO_2	SBA-15	*p6mm*	2.7	0.30	258	219
	MSU-H	*p6mm*	5.1	0.44	150	
	KIT-6	$Ia\bar{3}d$	3.9	0.41	220	
	SBA-15	*p6mm*	3.3–7.6	0.09–0.33	30–317	220, 221
	KIT-6	$Ia\bar{3}d$	4.9–7.2	0.14–0.25	103–346	
	KIT-6	$Ia\bar{3}d$	5, 11, 50	—	205	222
	KIT-6	$Ia\bar{3}d$	3.0–4.3	0.06–0.17	90–207	406
	Chiral silica film	*Chiral*	2.5–7.9	0.23–0.31	150–230	407
WO_3	SBA-15	*p6mm*	—	—	12.6	264, 265
	KIT-6	$Ia\bar{3}d$	7–8	—	48.2	
	SBA-15	*p6mm*	4.4–8.8	0.05–0.34	7.4–81.8	266
	KIT-6	$Ia\bar{3}d$				
	KIT-6	$Ia\bar{3}d$	3.5–20	0.18	54.3	267–269
ZnO	CMK-3, CMK-1	*p6mm*, $I4_132$	3.8–6.8	—	192–202	307
	CMK-3	*p6mm*	5.7	0.24	15–70	308–310
ZrO_2	SBA-15	*p6mm*	2.9, 27	0.57	220	233

[a] V_t: total pore volume. [b] S_{BET}: surface area calculated from the application of the BET equation to the nitrogen isotherm. [c] Do not remove the template.

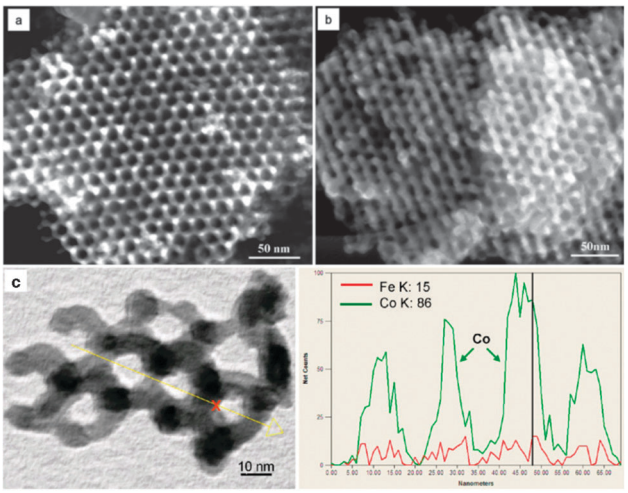

Fig. 3 HR-SEM images for (a) Co_3O_4 nanocasted by KIT-6, (b) Co_3O_4–$CoFe_2O_4$ composite transferred from Co_3O_4, and (c) line scan STEM-EDX elemental analysis of Co_3O_4–$CoFe_2O_4$ composite. [Reprinted with permission from ref. 90, copyright 2012 American Chemical Society.]

method''. By using this super lattice method, mesoporous CeO_2 with a crystalline framework was successfully synthesized.[112] Firstly, nearly monodisperse crystallized CeO_2 nanoparticles with a diameter of 5 nm were prepared. Then these CeO_2 nanoparticles were functionalized with 6-aminocaproic acid. The organic moiety was selected based on the principle that it possesses one terminal group (acid) which interacts with the nanoparticle surface and the other function (amine) that interacts with the surfactant. The nanoparticles and block copolymers co-assemble into mesostructured materials during the EISA process, finally resulting in the formation of material with 7.5 nm mesopores after removing the templates at 500 °C. The BET surface area of this mesoporous CeO_2 is as high as 160 $m^2\ g^{-1}$. Mesoporous tin oxide with pores sizes of 18–20 nm can also be prepared with 3.5 nm tin oxide nanoparticles and a polybutadiene-*block*-poly(ethylene oxide) PB-*b*-PEO block copolymer.[113] More recently, several other mesoporous architectures composed of metal oxides (TiO_2, ITO, Mn_3O_4, *etc.*) have

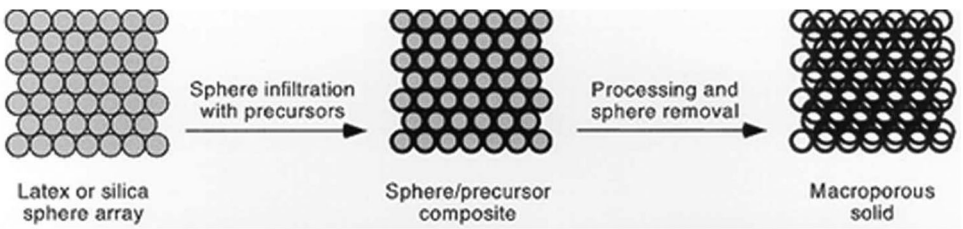

Fig. 4 Schematic synthetic process of the colloid crystal templating method. [Reprinted with permission from ref. 16, copyright 2006 Royal Society of Chemistry.]

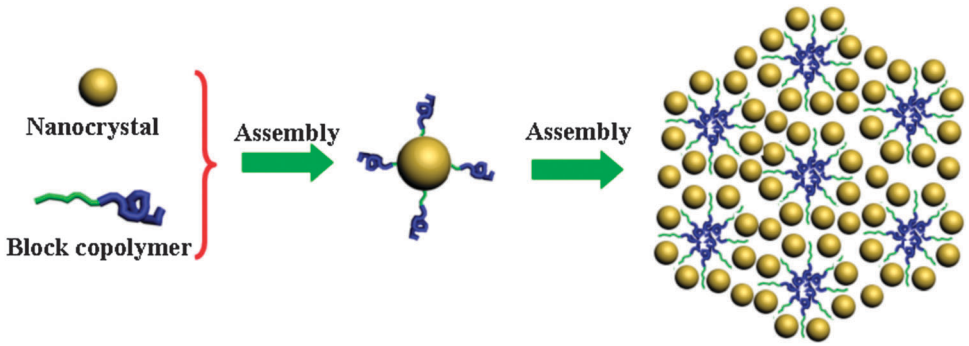

Fig. 5 Schematic illustration of the evaporation-induced self-assembly of nanocrystals into mesoporous materials by using block copolymers as templates.

been obtained from preformed building blocks, crystals and micelles.[114–116]

3. Controlling the properties of mesoporous non-siliceous oxides

3.1 Pore size control

There are several reliable methods for the synthesis of mesoporous silica materials with adjustable pore sizes. Choosing longer alkyl chain surfactants, increasing the temperature of the hydrothermal treatment, using large molecular weight block copolymers as templates, or adding swelling agents can yield mesoporous materials with larger pore sizes.[18] Some of these strategies are also suitable for the synthesis of mesoporous metal oxides.

The pore sizes of soft-templated ordered mesoporous metal oxides mainly depend on the hydrophobic volumes of the surfactant aggregates. When surfactants with small molecular weight are used as templates, mesoporous metal oxides with smaller pore sizes (normally below 4 nm) can be obtained. Mesoporous rare earth oxides with pore sizes between 2.5 and 3.0 nm have been synthesized using sodium dodecyl sulfate (SDS) as the template.[117] Hexadecylamine also can be used as the template to fabricate mesoporous metal oxides with a pore size around 2 nm.[118] Alternatively, large molecular block copolymers are used to synthesize mesoporous materials with large pore size. The commercially available PEO–PPO–PEO triblock copolymers were the first ones used for the synthesis of mesoporous metal oxides with stable mesostructures and large pore sizes.[27] The hydrophobic block segments contain several tens of repeat units, which is several times higher than the molecular surfactants. The hydrodynamic radii range from 6 to 10 nm. Therefore, the pore sizes of mesoporous metal oxides templated by block copolymers are larger than those obtained with low molecular weight surfactants. Mesoporous Al_2O_3 synthesized with Pluronic P123 as a template has a pore size of 4–7 nm,[119] compared with 1.0–2.7 nm for materials synthesized with SDS or cetyltrimethylammonium bromide (CTAB) as templates.[120] Diblock copolymers are always directing towards larger pore sizes compared with triblock copolymers with similar molecular weights or hydrophilic chain lengths. This is due to the fact that the latter tend to bending aggregation. Wiesner and coworkers[121] were the first to demonstrate the large pore size of aluminosilicates and silicates created by diblock copolymers PI-*b*-PEO. The class of diblock copolymers includes poly(hydrogenated poly-*b*-butadiene-coethylene)-*block*-poly(ethylene oxide) KLE[122–132] poly(isoprene)-*block*-poly(ethylene oxide) PI-*b*-PEO,[125,133,134] poly(styrene)-*block*-poly(ethylene oxide) PS-*b*-PEO,[135,136] and poly(butadiene)-*block*-poly(ethylene oxide) PB-*b*-PEO.[113] All of them can template mesopores with larger pore sizes which are of great interest for metal oxide synthesis. Fig. 6 shows the

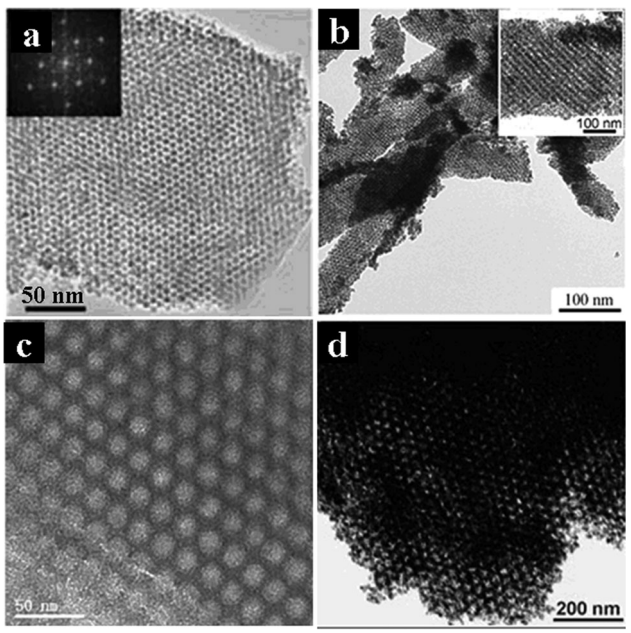

Fig. 6 TEM images of (a) mesoporous Al_2O_3 templated by KLE22 after treatment at 400 °C [reprinted with permission from ref. 122, copyright 2005 Wiley], (b) mesoporous α-Fe_2O_3 film templated by PI-*b*-PEO after treatment at 450 °C, the insert is a magnification [reprinted with permission from ref. 125, copyright 2006 Wiley], (c) mesoporous TiO_2 templated by PS-*b*-PEO after treatment at 600 °C in nitrogen, view from the [100] direction [reprinted with permission from ref. 136, copyright 2011 Wiley], and (d) mesoporous SnO_2 templated by PB-*b*-PEO after calcination [reprinted with permission from ref. 113, copyright 2005 Wiley].

mesoporous metal oxides templated by diblock copolymers with large mesopores.

Furthermore, in most cases, the small molecular surfactants can only yield disordered metal oxide mesostructures, and the frameworks are amorphous.[137–149] The main reason is that the metal oxides have a high nucleation-to-growth ratio, which makes the nanoparticles grow too big during the aging and thermal treatment process. Thus the primary ordered mesostructures are lost during the crystallization process, partly due to mass transport in the walls and partly due to the missing connectivity between the nanoparticles. There are two complementing solutions for this problem. One is to adjust the conditions of the hydrolysis–condensation chemistry in a way that the solid formation proceeds slower and in a more controlled manner so that the formed composite structures are better interlinked. This can later support the nucleation of the inorganic phase during the thermal template removal process. One way to achieve this is reduction of the water content in the recipes, for instance, by addition of some alcohol[150] or by using ionic liquids.[151] The other possibility is the use of templates with high molecular weight as mentioned above. The larger hydrophilic segments result in thicker pore walls, which can maintain the ordered mesostructures during the thermal treatment process.

Adding organic swelling agents is an important way to expand pore sizes of mesoporous silicates. The hydrophobic organic species can be solubilized inside the hydrophobic regions of surfactant micelles. Although many successful examples have been reported in mesoporous silicate synthesis, for metal oxides, there are very few cases reported, yet.[152] This is either attributed to the EISA method used for metal oxide synthesis which is not easily compatible with the use of swelling agents, or the low structural ordering present anyway which can then be completely destroyed by the additives. Malfatti *et al.*[152] used poly(propylene glycol) (PPG) to swell the pore size of mesoporous TiO_2 templated by Pluronic F127 ($EO_{106}PO_{70}EO_{106}$). However, PPG only swells the F127 micelles at lower concentrations, while at high concentrations, it would induce a phase separation. The obtained TiO_2 materials possess a bimodal pore size distribution with a mesopore size tunable between 13 and 18 nm.

The hard-templating method usually limits the pore size of metal oxides to less than 7 nm, due to the limit in the thickness of walls – which determines the width of the pores of the replica – of the hard templates.[37,82,153] Efforts to prepare large and ordered porous metal oxides by the hard-templating method have thus focused on the synthesis of ordered mesoporous silica templates with thick walls. Such syntheses have proven to be very difficult.[16,64] Jiao *et al.*[154] demonstrated that it is a possible to generate mesoporous NiO with two pore sizes (3.3 and 11 nm) by controlling the temperature of the hydrothermal reaction used for the KIT-6 silica template. The presence of the large pore does not depend on the synthesis of a template with thick walls, but instead arises because one or the other of the two sets of the mesopore system in the template KIT-6 are filled. By varying the KIT-6 synthesis conditions, hence the degree of microporous bridging between the two sets of mesopores, it is possible to control the fraction of the different types of pores. More bridging leads to fewer large pores until only small pores remain. Tüysüz *et al.*[155,156] found the same phenomenon in the preparation of mesoporous Co_3O_4 with silica templates KIT-6 that had been synthesized at different temperatures.

3.2 Crystallinity

The amorphous nature of the pore walls of most mesoporous metal oxides, which lead to only poor thermal and mechanical stability, restrict the range of applications of these materials. In contrast, a crystallized wall structure can be expected to provide better thermal and mechanical stability, as well as superior electrical and optical properties. In addition, the presence of crystallized wall structures could cause the appearance of specific electronic states and/or lattice defects that are frequently responsible for specific catalytic properties and that are notably absent in amorphous materials. For example, when mesoporous titanium dioxide is applied in photocatalysis, the amorphous regions are known to be trap sites for the recombination of photo-excited electrons and holes,[157] limiting the device efficiency. Despite many efforts, up to now it remains a major challenge to convert the amorphous framework of the as-synthesized materials to crystalline materials while simultaneously retaining the original mesostructures.[158] Heat treatment, which typically is used for crystallizing amorphous materials, also leads to higher mobility of atoms, and this, together with the movement of atoms during crystallization, leads to loss of the mesostructure. The calcination conditions are chosen by considering the rate of surfactant combustion, extent of local thermal extremes due to combustion, the rate of nucleation, the rate of crystal growth, and so on.

To prevent the loss of structural order, a carbon protected crystallization procedure can be applied to synthesize mesoporous metal oxides with the crystalline framework. Domen *et al.*[159] filled the carbon precursor into the pores of 2-D hexagonal mesoporous Nb–Ta mixed oxide. Then, the sample filled with the carbon scaffold was crystallized by calcination in an inert atmosphere followed by removal of the carbon by calcination in air. Recently, Wiesner and coworkers[133] reported a so-called CASH (''combined assembly by soft and hard'') method to fabricate ordered mesoporous group 4 transition metal oxides with large pore size and a highly crystalline framework (Fig. 7). In this case, an amphiphilic diblock copolymer PI-*b*-PEO was used as a structure directing agent. The diblock copolymer has sp^2-hybridized-carbon in the hydrophilic chain, which is transformed *in situ* into a carbon scaffold inside the pore channels. This method can be applied to synthesize mesoporous TiO_2 with PS-*b*-PEO[136] or a triblock copolymer Pluronic P123 ($EO_{20}PO_{70}EO_{20}$) as a template.[160]

The second generic method for the synthesis of mesoporous metal oxides with crystalline wall structure is the hard-templating pathway, in which inorganic precursors are filled into pre-formed ordered mesoporous silica or carbon templates that are removed in the subsequent steps.[16,37,64] For this nanocasting method, heat treatment at elevated temperatures

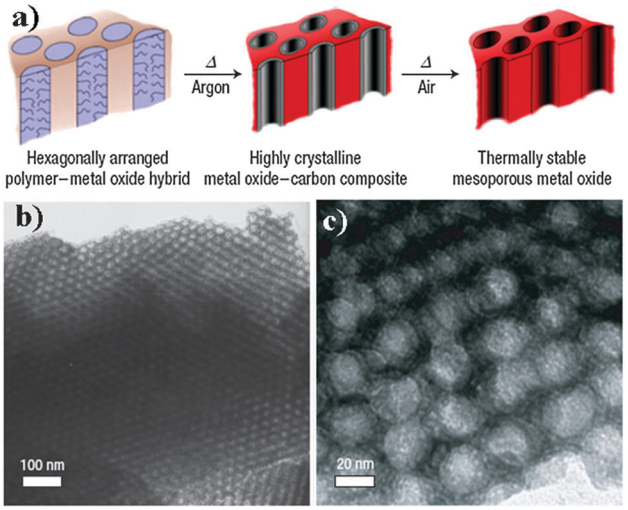

Fig. 7 (a) Schematic representation of the CASH method; TEM images of as-made Nb_2O_5 (b) and crystalline mesoporous Nb_2O_5 synthesized using the CASH method (c). [Reprinted with permission from ref. 133, copyright 2008 Nature Publishing Group.]

is possible without structural collapse, and highly crystalline materials can be obtained. The precursors are introduced into the pore channels in the form of either a heteropolyacid or a nitrate for most metal oxides. The inorganic precursors inside the nanospaces of mesoporous materials can decompose and grow into crystalline oxides. Many efforts have been focused on the synthesis of mesoporous metal oxides with single crystal domains.[82,161,162] The Zhao group[161] reported a simple one-step nanocasting route to prepare ordered single crystalline In_2O_3 nanowire arrays with hexagonal and cubic mesostructures. Zhou and coworkers[82] demonstrated that those metal oxides with a cubic symmetry, synthesized by a 'solid–liquid method', can form porous single crystals.

High pressure synthesis is another method which can result in the formation of crystalline phases, which is, however, seldom used. Very recently, a carbon protection, high pressure method was used to synthesize periodic mesoporous silica with crystalline channel walls.[163] A periodic mesoporous coesite has been obtained by a modified nanocasting route from periodic mesoporous silica SBA-16. In the first step, the SBA-16 was infiltrated with molten mesophase pitch as a carbon source. Then the mesophase pitch was carbonized at 900 °C in an inert atmosphere. The silica–carbon composite was pressurized at 12 GPa to convert amorphous silica to the coesite framework, before removing the carbon protector at 500 °C in air. The BET surface area of this kind of coesite reached 278 $m^2\ g^{-1}$. Based on this method, mesoporous coesite with single crystal framework can also be synthesized.[164]

The use of pre-formed and fully crystalline nanoparticles as building blocks to assemble mesoporous frameworks is another effective route to obtain crystalline structures, as mentioned in the previous sections.

3.3 Phase control

The mesostructures of metal oxides are an important characteristic feature of this class of materials, due to their influence on mass transfer and adsorption properties. The phase of mesostructured metal oxides obtained by soft-templating can be rationally controlled by tuning organic–inorganic interactions and cooperative assembly of metal species and templates, in a manner quite similar to what is known for mesoporous silica materials.[18,165] The decisive factor governing the formation of specific mesophases is the organic–inorganic composite liquid crystal phase, which is influenced by the hydrophilic/hydrophobic volume ratios. For nanocast mesoporous metal oxides, on the other hand, the mesostructures are simply determined by the template. The resulting mesostructured metal oxide is in most cases the negative replica of the mother template, the most well-known exception being the replication of KIT-6, where, depending on the conditions, both or only one of the enantiomeric pore systems of the parent might be replicated.

By now, many different mesostructure phases are reported for mesoporous metal oxides including those with the space groups $p6mm$[27,29,56,117,119,133,166–186] $Ia\bar{3}d$,[118] $Im\bar{3}m$,[124–126,128,129,187–189] $Fm\bar{3}m$,[122,127,170] $P6_3/mmc$,[172,190,191] $R\bar{3}m$,[192] and primitive cubic.[136,193] Fig. 8 shows transmission electron microscopy (TEM) images of nanocast mesoporous Co_3O_4 with different mesostructures. Large pore mesoporous silicas are becoming more and more popular as hard templates due to their three dimensionally connected and open pore structures, making them more easy to be filled with inorganic precursors.

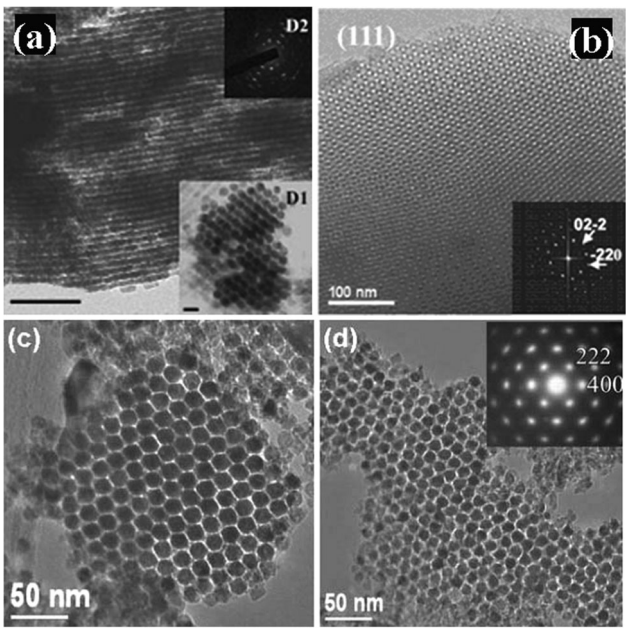

Fig. 8 TEM images of nanocast mesoporous Co_3O_4 with different mesostructures. (a) Viewed from [110] and [100] (insert D1) directions of $p6mm$ structure [reprinted with permission from ref. 37, copyright 2003 Wiley], (b) viewed from the [111] direction of $Ia\bar{3}d$ structure [reprinted with permission from ref. 79, copyright 2004 American Chemical Society], (c) viewed from the [111] direction of $Fm\bar{3}m$ structure [reprinted with permission from ref. 82, copyright 2007 Royal Society of Chemistry], and (d) viewed from the [111] direction of $Im\bar{3}m$ structure [reprinted with permission from ref. 82, copyright 2007 Royal Society of Chemistry]. The insets of D2 and (d) are SAED patterns and that of (b) is the corresponding Fourier diffractogram.

SBA-15 with *p6mm* structure and KIT-6 with $Ia\bar{3}d$ structure with pore sizes of around 7–10 nm are the most often used hard templates. Mesoporous silicas with a spherical pore shape are considered as difficult to be used as hard templates because their small window sizes are limits for the precursors to fully penetrate the pore system and thus later form a less coherent mesostructured negative replica. Up to now, many mesostructures with space groups already found in mesoporous silica, such as $Pm\bar{3}n$, $Pn\bar{3}m$, $Fd\bar{3}m$, and $Pm\bar{3}m$, have not been obtained as mesoporous metal oxide compositions.

4. Compositions

As discussed in the previous section, several quite versatile methods have been invented for the preparation of mesoporous metal oxides with different composition. In the following, the different compositions accessible today and the most salient features of these materials will be discussed.

4.1 Alumina

High surface area alumina is especially important as an industrial catalyst and a support, due to its high hydrolytic stability and the range of point of zero charge it can have, which facilitates loading it with different metal species.[194] Much effort has been invested in the synthesis of ordered mesostructured forms of alumina with surfactants as templates.[23,195,196] However, in all of these approaches, the obtained products collapsed upon the removal of surfactants.

Most attempts for the synthesis of mesoporous alumina rely on the aqueous solution method. The first successful synthesis of mesoporous alumina was reported by Bagshaw and Pinnavaia in 1996.[137] The alumina was prepared by using poly-(ethylene oxide) based nonionic surfactants as the template. The pore size of the obtained MSU materials after calcination at 500 °C to remove the template is between 4.0–8.0 nm, and the surface area is around 425–535 $m^2\ g^{-1}$. This kind of mesoporous alumina has a wormhole-like pore structure. Almost at the same time, Vaudry and Davis[197] reported a highly thermally stable (up to 800 °C) mesoporous alumina with a specific surface area as high as 710 $m^2\ g^{-1}$ and narrow pore size distribution by reacting aluminum alkoxides with carboxylic acids in low-molecular-weight alcoholic solvents with controlled amounts of water. The absence of an ordered mesostructure may suggest that the surfactants do not really act as templates in this synthesis. Yada *et al.*[198] first reported the formation of ordered mesostructured alumina with SDS as a template. An alumina-based composite material with hexagonal mesostructure can be obtained by the homogeneous precipitation method. However, the mesostructure collapsed after removing the template. Alumina with a pore size as large as 14.0 nm was accessible following this route, but unfortunately the pore structure after template removal was also disordered. Then Vaudry *et al.* reported a variety of synthesis pathways leading to thermally stable mesoporous aluminum oxide phases, based on co-assembly of inorganic species and the surfactant. All the mesostructured materials were obtained in aqueous media by hydrolysis and condensation of different inorganic aluminum reactants involving monomeric cations such as $[Al(H_2O)_6]^{3+}$ and/or oligomeric cationic species such as Keggin aluminum clusters, in the presence of single (anionic or non-ionic) or mixed (cationic–anionic) surfactant micelles, at pH values lower than the isoelectric point of alumina, typically 8–9. Selected anionic surfactants were dodecyl sulfate or carboxylic acids, optionally mixed with small amounts of CTAB, while the non-ionic surfactants belong to the polyethylene glycol-phenyl ether and the amine-*N*-oxide families. Most of the mesophases exhibited thermally stable and regular porous structures. Strongly depending on the synthesis and calcination conditions, their mean pore diameters are between 0.8 and 6.0 nm and their specific surface areas are between 100 and 810 $m^2\ g^{-1}$. The wall structure of these aluminas, however, was amorphous in all cases.

In contrast to this, the Pinnavaia group found a stepwise reaction protocol leading to mesostructured forms of γ-Al_2O_3 with lathlike framework morphologies from aluminum salts in the presence of both triblock PEO–PPO–PEO and diblock $RO(EO)_xH$ surfactants as structure directing agents. The crystallized walls of the resulting lathlike MSU-γ aluminas highly improved their hydrolytic stability.[199,200] Firstly, a mesostructured alumina with a wormhole like structure and amorphous pore walls was assembled through the hydrolysis of Al_{13} oligocations and hydrated aluminum cations in the presence of nonionic surfactants. Then the walls of the initial mesostructure were transformed in a second hydrolysis step at a higher temperature to a surfactant-boehmite mesophase, denoted as MSU-S/B, with a framework made of lathlike boehmite nanoparticles. Finally, the intermediate boehmitic framework was converted to crystalline γ-Al_2O_3. The first example of ordered mesoporous alumina synthesized using a block copolymer as a template in aqueous solution was reported by the Somorjai group.[166] An ordered hexagonal alumina with amorphous walls was synthesized through a sol–gel route under strict control of the hydrolysis and condensation of reagents.

A non-aqueous method to synthesize mesoporous alumina was introduced after the success in the synthesis of mesoporous silica. In 1998, the Stucky group[27,29] achieved a series of mesoporous metal oxides and mixed oxide materials using a triblock copolymer as the template *via* the EISA method. By employing aluminum alkoxide (*e.g.* $Al(OC_4H_9)_3$) as the main inorganic precursor and $AlCl_3$ as the pH 'adjustor' and the hydrolysis–condensation 'controller', partly ordered mesoporous alumina was fabricated by the Zhao group.[201] By utilizing the dip-coating technique, Sanchez and coworkers[122] studied the formation of mesoporous 3-D cubic alumina thin films with diblock copolymer KLE as a template. In this case, the ability to stabilize γ-Al_2O_3 nanoparticles in the form of a well-ordered mesostructured network is attributed to the stability of the KLE template above the dehydration temperature of the inorganic phase. When the treatment reaches the KLE decomposition temperature at 350 °C, the amorphous inorganic dehydrated framework is rigid enough to prevent the mesostructure from collapsing. Above 400 °C, progressive crystallization by nucleation and growth slowly takes place. Recently, Yan *et al.*[119,167] reported a simple sol–gel route with triblock copolymers (Pluronic P123, and

F127) as soft templates under controlled conditions. Using this strategy, a series of highly ordered mesoporous aluminas with 2-D hexagonal structure was obtained (Fig. 9). More importantly, these mesoporous aluminas exhibited a high thermal stability up to 1000 °C without losing their ordered mesostructures. Based on this method, Jaroniec *et al.*[168] prepared a series of metal oxide loaded mesoporous aluminas with metal molar percentages (the ratio of metal to aluminum) as high as 20%. They also found that the pore size of this kind of alumina can be tailored by controlling the acid concentration in the synthesis mixture.[169] The pore size can be tuned from 4.0 to 15.5 nm by just adjusting the molar ratio of acid to the metal species. Recently, mesoporous alumina with $Im\bar{3}m$ cubic structure has been synthesized by using a partially chelated acetyl-acetonato complex of aluminium tri-*sec*-butoxide without any control of external factors like temperature and humidity with Pluronic F127 as a template.[187]

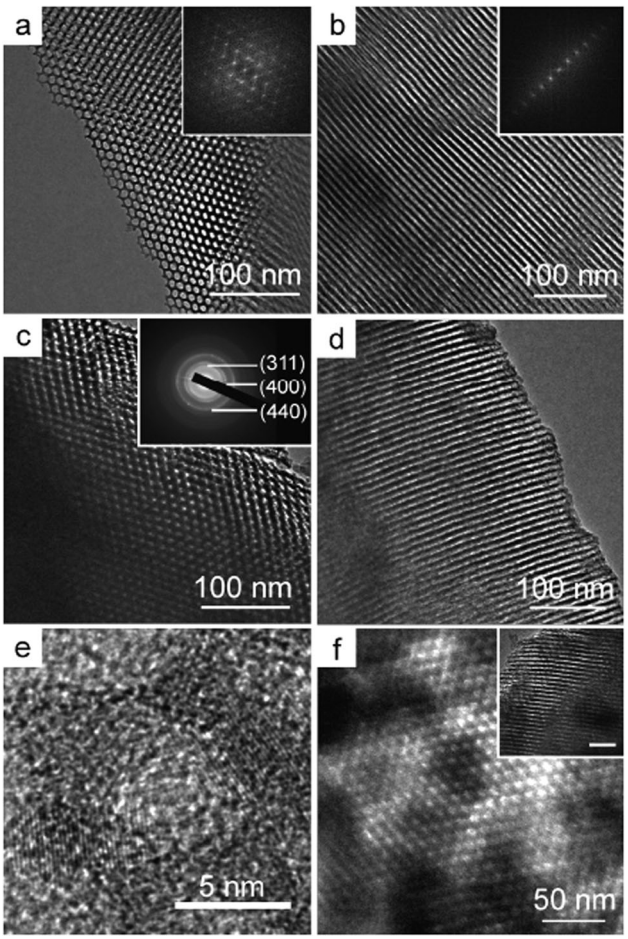

Fig. 9 TEM images of ordered mesoporous alumina synthesized using a triblock copolymer as a template. (a) and (b) Mesoporous alumina calcined at 400 °C viewed along [001] and [110] orientations (FFT diffractogram inset), (c) and (d) mesoporous alumina calcined at 900 °C viewed along [001] and [110] orientations (the inset in (c) is the corresponding SAED pattern), (e) HRTEM image of mesoporous alumina calcined at 900 °C, (f) TEM image of mesoporous alumina calcined at 1000 °C viewed along [001] orientation (the inset is TEM image viewed along [110] orientation). The bars are 50 nm for insets. [Reproduced with permission from ref. 119, copyright 2008 American Chemical Society.]

Mesoporous alumina can also be synthesized by the nanocasting method with porous carbons as templates. The Schüth group[202] used carbon aerogel as a hard template to prepare a glassy, amorphous, disordered mesoporous alumina with large pore volume (1.55 $cm^3\ g^{-1}$), high surface area (365 $m^2\ g^{-1}$), and controllable pore sizes. The Zhang group[203] reported a repeated nanocasting route to synthesize ordered mesoporous alumina with crystalline pore wall structure and the SBA-15 mesostructure. Firstly, high quality CMK-3 mesoporous carbon material was nanocasted with SBA-15 as a hard template. Then CMK-3 was used again as a hard template for mesoporous alumina. The mesoporous carbon does not only act as a rigid hard template but also effectively preserves the ordered mesostructure during the crystallization of the amorphous framework walls through a stepwise calcination procedure. Recently, the Zhao group[87] used a surface functionalized mesoporous carbon, which was synthesized by soft-templating and had a bimodal pore size distribution, as a hard template to controllably synthesize ordered mesoporous γ-Al_2O_3 with variable pore architectures and high mesoporosity at low temperature (500 °C). It was found that the impregnation amount of alumina precursor can be a key factor to tailor the porosity of alumina. If the carbon template is impregnated once or twice, only the hexagonal pore walls are filled, and a replica in the form of SBA-15-like alumina is produced. If the template is impregnated three or more times, almost both of the two types of mesopores are filled, which produces alumina close to the inversed structure of the carbon template.

4.2 Transition metal oxides

Transition metal oxides have various applications in catalysis because of their redox activity. Mesostructured transition metal oxides with large and uniform pore size and high surface area, which will lead to fast diffusion to the active sites during catalysis, would be very attractive. However, the first attempts aimed at synthesizing mesoporous transition metal oxides were not very successful. The mesostructures were thermally unstable and their structures collapsed readily upon surfactant removal during calcination. However, with the development of new methods and templates for the preparation of mesoporous materials, especially the introduction of large block copolymers as a new kind of template, and the nanocasting method, most transition metal oxides with mesostructures can be attained now.

4.2.1 IV B group metal oxides

4.2.1.1 Titania. Different allotropes of titania (TiO_2) have been extensively studied because of their unique electronic and optical properties as well as potential applications in the fields of lithium-ion batteries, photocatalysis, DSSC, catalysis, sensing and biotechnology.[204–207] Most of these applications are strongly dependent on the surface structure, crystallization degree, specific surface area as well as large and tunable pore sizes. Ordered mesoporous titania possesses extraordinarily large surface areas and well-arranged pore channels, which do not only greatly maximize the active surfaces, but also promote the adsorption capabilities, as well as facilitate mass transfer within the pore

system. Much work using various strategies has been invested in the synthesis of ordered mesoporous titania to replace the dense materials.[208]

In 1995, Antonelli and Ying[24] first reported a thermally stable ordered mesoporous TiO_2 material based on a ''ligand-assisted'' self-assembly strategy. In their synthesis, tetradecylphosphate was used as a template and acetylacetone was employed as a ligand to decrease the hydrolysis rate of titanium isopropoxide through the formation of titanium acetylacetonate tris-isopropoxide. After calcination in air at 350 °C, ordered hexagonally packed mesoporous TiO_2 materials were obtained with BET surface areas of $\sim$200 m^2 g^{-1} and pore sizes of $\sim$3.2 nm. However, this strategy was just successful with surfactants with phosphate head groups, but not with cationic surfactants or other anionic surfactants, such as those with carboxylate or sulfate head groups. The phosphorus from the template was bound so strongly to titanium that it could not be fully removed by either calcination or solvent extraction. Since these materials had considerable amounts of phosphorus retained in them, they are better designated as titanium oxo-phosphates rather than pure titania. This limits its possible use as a catalyst or a support. Thieme and Schüth[209] used a non-ionic surfactant (Dodecanol + 5 EO units) as the soft template to synthesize a high surface area (350 m^2 g^{-1}) mesoporous titanium oxo phosphate with disordered structure.

The synthesis of phosphorus free mesoporous TiO_2 material was first reported by Antonelli[210] using organic amine as a template. Nitrogen adsorption studies of an as-synthesized sample gave an isotherm similar to MCM-41 with a surface area of 710 m^2 g^{-1} and a narrow pore size distribution centered at $\sim$2.7 nm. When this material was subjected to heat treatment, the anatase phase was formed accompanied by a loss of mesoscopic order, leading to a low surface area of 180 m^2 g^{-1}. Interestingly, when the length of the carbon chain in the organic amine was increased from 12 to 18 carbon atoms, no increase in pore size was observed. Later, Gedanken and coworkers[147] demonstrated an ultrasound irradiation assisted self-assembly process for the preparation of well crystallized mesoporous TiO_2 with a large surface area of 180 m^2 g^{-1} by using octadecylamine.

In 1998, Yang *et al.*[27,29] first used amphiphilic block copolymers as structure-directing agents to prepare mesoporous metal oxides through the EISA process (Fig. 10a and b). The relatively weak coordination interactions at the inorganic/organic interface promote the cooperative assembly of inorganic/copolymer mesostructures, yielding thermally stable hybrid mesostructures. Ordered hexagonal mesoporous TiO_2 with a surface area of $\sim$205 m^2 g^{-1} and a pore size of 6.5 nm was obtained by using titanium tetrachloride ($TiCl_4$) as a precursor and triblock copolymer Pluronic P123 as a template after calcination at 400 °C for 5 h in air. Cubic mesophases of mesoporous TiO_2 are preferred when block copolymer Pluronic F127 and $EO_{75}BO_{45}$ ($HO(CH_2CH_2O)_{75}(CH_2CH(CH_3CH_2)O)_{45}H$) are used as the structure directing agents. Since this synthetic strategy relies on a non-aqueous pathway, the hydrolysis and condensation rates of titanium precursor are very low.

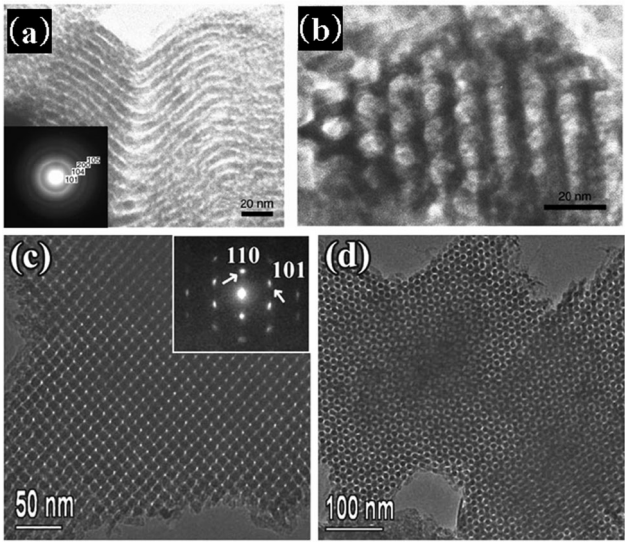

Fig. 10 (a and b) TEM images of 2-D hexagonal mesoporous TiO_2 synthesized with P123 as a template. [Reproduced with permission from ref. 27, copyright 1998 Nature Publishing Group.] (c and d) 3-D cubic mesoporous TiO_2 synthesized with KIT-6 as a hard template. [Reproduced with permission from ref. 221, copyright 2009 American Chemical Society.]

Thus, crystallization of bulk oxide is avoided. Moreover, there is no need for use of stabilizing agents thanks to the direct weak coordination interactions between Ti^{4+} and the polymer. Such a method could successfully also be applied to prepare mesoporous TiO_2 films.[211] Recently, an aqueous route based on EISA was also exploited to prepare thick and crack-free mesoporous TiO_2 films by capillary dip-coating.[212,213]

It is well-known that the hydrolysis and condensation rates of titanium precursors are very fast, which leads to rapid formation of a dense inorganic network, yielding poorly ordered mesostructured TiO_2 materials. One suitable solution is the addition of complexing molecules or acids as stabilizing agents. Sanchez and coworkers[50,54,214] have performed a series of studies on controllable synthesis of highly ordered mesoporous TiO_2 films with a nanocrystalline framework. Fig. 11 schematically illustrates the typical EISA process for the block copolymer-templated preparation of highly ordered mesoporous TiO_2 films. In their synthesis, titanium chlorides and titanium alkoxides were used as the inorganic source, ethanol was used as the solvent, and block copolymers were used as the template. Importantly, controlled quantities of water were added to the solutions, and HCl was employed as well. These conditions cause controlled hydrolysis of the inorganic moieties, resulting in hydrophilic species with enhanced interactions with the polar portion of the template. Moreover, water contributes to increase the polarity of the medium, facilitating template folding. The added or *in situ* generated HCl controls hydrolysis and condensation of the titanium precursor and can subsequently be eliminated by evaporation. For these preparations, also details of the processing are important. First, the mixed precursor solutions are transferred to a substrate. Second, the films are subjected to a humidity aging process to facilitate the cooperative

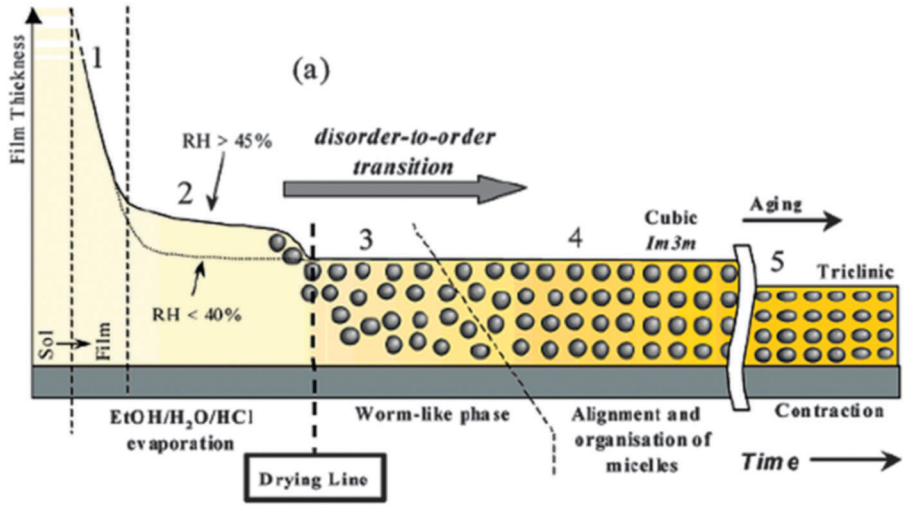

Fig. 11 Schematic representation of the EISA process used to synthesize ordered mesoporous materials. [Reprinted with permission from ref. 54, copyright 2003 American Chemical Society.]

assembly between Ti species and block copolymer molecules, resulting in a robust and highly organized mesostructure. After a two-step thermal treatment – gelation at a lower temperature and subsequent calcination at a temperature above 300 °C – the block copolymer can be completely removed from the gradually solidified film, and mesoporous TiO_2 films are obtained. The *in situ* analysis of the structural evolution related to the advancement of the evaporation process led to a deep understanding of the role of each of the variables involved, allowing the reproducible formation of transparent, crack-free, and high surface area mesoporous TiO_2 films.[191,192,215,216] Smarsly *et al.*[130] used KLE diblock copolymer as the template to synthesize highly crystalline mesoporous TiO_2 thin films with a well-defined contracted $Im\bar{3}m$ mesostructure and a large pore size of about 10 nm. Fan *et al.*[56] modified this method by employing acetic acid as a complexing agent to control the condensation kinetics of titanium alkoxides. The obtained mesoporous titanias show highly organized mesostructures, a pore size of ~5.0 nm and a large surface area of 191 $m^2\ g^{-1}$.

The aqueous solution approach, which has been widely used in the synthesis of mesoporous silicates, is normally considered as an ideal method, because it is simple and leads to highly ordered mesostructures with few defects, easily tailored pore sizes, and well-controlled morphologies. Compared to the EISA method, the aqueous route shows better reproducibility and is principally not limited with respect to batch size, which makes it suitable for industrial production well. However, because the hydrolysis and condensation rates of titanium precursors are so fast, only few studies have reported the successful preparation of ordered mesoporous TiO_2 by the aqueous route. Sakai and coworkers[127,128] demonstrated that ordered mesoporous titania with a crystalline wall can be prepared by using titanium oxysulfate sulfuric acid hydrate ($TiOSO_4{\cdot}xH_2SO_4{\cdot}xH_2O$) as a precursor and the cationic surfactant CTAB as a structure directing agent at 160 °C.[217,218] In this case, at 160 °C, the intermediary compound obtained from titanium oxysulfate sulfuric acid hydrate was bound to the hydrophilic group of CTAB by the strong interaction, thus titanium hydroxide oxide ($TiO(OH)_2$) was quickly formed. Upon further treatment, titanium hydroxide oxide ($TiO(OH)_2$) was crystallized to anatase. In this process, bromide ions (Br^-) played the role of retaining the anatase crystal structure and surfactant molecular assemblies keeping its crystal size small. The obtained mesoporous anatase showed a high surface area of 262 $m^2\ g^{-1}$, but a very low thermal stability.

It is well-known that high crystallinity of TiO_2 with a low degree of surface defects is one of the critical factors in improving its performance in different applications. Generally speaking, high crystallinity requires high calcination temperature. However, thermal treatment of typical mesoporous TiO_2 to transform the pore walls into crystalline structures usually leads to undesirable grain growth and a total collapse of the ordered mesoporous network. Recently, Wiesner and coworkers[133] reported the synthesis of well-organized, highly crystalline mesoporous transition metal oxides using an amphiphilic diblock copolymer PI-*b*-PEO as the structure directing agent that contains a hydrophilic block and an sp^2-hybridized-carbon-containing hydrophobic block. The approach combines advantages of both soft structure directing assemblies and hard-templating chemistries, so that it is referred to as ''combined assembly by soft and hard'' templating (CASH). In the CASH method, firstly, equal molar amounts of titanium isopropoxide and titanium chloride are added to a solution of the polymer in tetrahydrofuran (THF). The metal oxide sol selectively swells the hydrophilic PEO part of the block copolymer. Secondly, casting of the block copolymer–metal oxide solution in air and allowing the volatiles to evaporate results in an amorphous hybrid material. Thirdly, to obtain highly crystalline materials, the as-made films are subsequently heat treated under argon in a tube furnace to 700 °C. During this process, the PEO chain is pyrolyzed and the metal oxide crystals nucleate, grow and sinter into a framework forming the pore walls. At the same time, part of the PI chain is converted to an

amorphous carbon that lines the walls of the resulting cylindrical pores. This *in situ* carbon is sufficient to act as a rigid support to the mesostructured oxide walls, preventing collapse when heat-treated to temperatures required for obtaining highly crystalline materials. At last, the carbon can subsequently be removed by heating the material in air, leaving a well-organized, highly crystalline mesoporous TiO_2. This is quite similar to the method used by Domen and coworkers.[159] In that case, the carbon scaffold was post-deposited in the pore system prior to crystallization of the inorganic materials. Zhao and coworkers[160] demonstrated a simple surfactant/sulfuric acid carbonization method to synthesize ultra-stable ordered mesoporous titania with highly crystalline anatase frameworks and a BET surface area as high as 193 $m^2\ g^{-1}$. They used H_2SO_4 as a catalyst to carbonize the amphiphilic triblock copolymers (Pluronic P123, F127 or F108 ($EO_{132}PO_{50}EO_{132}$)). The *in situ* produced carbon could support the TiO_2 framework during the high temperature crystallization. An alternative route to resolve the problem of thermal stability is addition of amorphous stabilizing components, such as SiO_2,[184] or carbon[185,186] into the mesostructured TiO_2 frameworks. However, the presence of these additional compounds is unfavorable in many applications.

Since small molecular surfactants (*e.g.* CTAB and organic amine) and the commercial PEO–PPO–PEO triblock copolymers are normally used as templates in soft-templating, they usually lead to mesoporous titania with pore sizes smaller than 10 nm due to the limitation of the hydrophobic chain length. This may by limiting for applications in which larger pores are required. The synthesis of ordered mesoporous TiO_2 materials with large pores has thus become a subject of extensive research. Such larger mesopores could accommodate large guest objects, such as in adsorption/immobilization of biomacromolecules or immobilization of metal nanoparticles for catalysis, without blocking the pore channels. Recently, Zhao and coworkers[136] demonstrated a novel ligand-assisted assembly method for the synthesis of highly ordered and crystalline mesoporous titania with uniform large pores using titanium isopropoxide (TIPO) as a precursor, a lab-made diblock copolymer PS-*b*-PEO as a soft template and THF as a solvent. The acetylacetone was employed as a coordinating ligand during the EISA process to retard the hydrolysis and condensation of titanium isopropoxide by stabilizing the hydrolyzed Ti species *via* chelation, which makes the assembly process more controllable. Ordered mesoporous titania can be obtained with primitive cubic mesostructure, highly crystallized anatase framework, large pore size of 16 nm, high BET surface areas of $\sim$112 $m^2\ g^{-1}$, and high thermal stability. Ortel *et al.*[189] reported well crystallized mesoporous TiO_2 films with a tunable pore size of 7.6–21.1 nm using a series of amphiphilic triblock copolymers poly(ethylene oxide)–polybutadiene–poly(ethylene oxide) (PEO–PB–PEO) with different sizes as the templates.

Another widely used process for the synthesis of mesoporous TiO_2 is the hard-templating method. Hard templates, such as ordered mesoporous silica, which can resist high temperatures and are easily removed, act as rigid supports for the mesostructured oxide, preventing collapse when heat-treated to temperatures required to obtain highly crystalline materials. Kim *et al.*[219] first demonstrated a facile synthesis of mesoporous TiO_2 materials with highly ordered mesostructures and crystalline frameworks using different mesoporous silica templates such as SBA-15 (2-D hexagonal *p6mm*), MSU-H (2-D hexagonal *p6mm*), and KIT-6 (bicontinuous cubic $Ia\bar{3}d$) and a freshly synthesized titanium chloride solution as a precursor. The titanium chloride solution was fabricated by first mixing $Ti(OEt)_4$ with water, resulting in a white precipitate, followed by adding HCl (35 wt%) to dissolve the precipitate to a clear sol. The mesoporous TiO_2 materials, hard templated with this precursor solution, had well-developed, regular mesopores, high surface areas and crystalline anatase frameworks. In 2009, Zhou and coworkers[220,221] prepared porous monocrystalline rutile TiO_2 and porous anatase nanocrystal $Ti(Si)O_2$ materials, using SBA-15 or KIT-6 as a hard template and a freshly synthesized titanium nitrate or titanium chloride solution as a precursor (Fig. 10c and d). Ren *et al.*[222] investigated lithium intercalation in ordered 3-D mesoporous anatase which had been obtained from a hard template. The structural changes of mesoporous anatase are similar to those observed for nanoparticles, with continuous Li insertion into tetragonal anatase up to $Li_{0.05}TiO_2$, then a two-phase process between anatase and orthorhombic $Li_{0.45}TiO_2$, followed by continuous insertion into the orthorhombic phase up to $Li_{0.96}TiO_2$. Despite the intrinsic porosity of the mesoporous phase, the volumetric capacity is higher than the best capacities reported for nanoparticulate anatase previously, a two-fold increase being observed at the highest rates (24 A g^{-1}). The rate capability is better than for disordered mesoporous anatase, even if the latter is metalized, suggesting that the ordered pore structure is important for achieving high rate capability.

4.2.1.2 Zirconia. Zirconia (ZrO_2) has received considerable attention because of its high thermal stability, high resistance against corrosion and acid–base bifunctional activity.[223,224] Owing to these features, zirconia-based materials are potentially applicable in redox and photo-catalysis and in conventional catalysis, both as catalysts and as supports. Zirconium oxide is of particular interest also for acid catalysis.[223] It contains both weakly acidic and basic surface sites, providing high activity in reactions requiring acid–base bifunctional catalysts,[225] and after modification with sulfate it can be highly acidic.[226]

The soft-templating method is the most common way to fabricate mesoporous ZrO_2 materials, in which small molecular weight surfactants (such as amine, carboxylate, sulfate, and CTAB) and commercially available block copolymers are used as the templates. The Schüth group[227,228] first used zirconium sulfate as the zirconium source and alkyltrimethylammonium bromide as the surfactant to synthesize highly ordered zirconium-based mesoporous materials. Hudson *et al.*[229,230] used amines as a scaffolding agent to produce mesoporous ZrO_2 with high surface area and disordered mesostructures. Ying *et al.*[149] synthesized mesostructured zirconium oxide *via* the covalent-bond approach by using amphiphilic compounds with a variety of headgroups (anionic and nonionic) and trial group chain lengths (1–18 carbons) as templates. However, the

access to stable, well-defined mesoporous structures was highly dependent on the nature of the head groups. Anionic surfactants with phosphate, carboxylate, sulfate, and sulfonate headgroups led to disordered hexagonal and/or layered phases. After calcination, mesoporous zirconia with high surface area can be obtained by using phosphate as a template, due to the stabilizing effect of phosphate headgroups in a similar manner as described by Ciesla *et al.*[210] By using a non-aqueous synthesis method, Ozin and coworkers[231] obtained ordered mesoporous ZrO_2 and several other transition metal oxides. Block copolymers also have been used as the template to fabricate mesoporous ZrO_2 with large pores through the non-aqueous EISA route.[27,29] Sanchez *et al.*[214] prepared multi-scale crystalline mesoporous ZrO_2 spheres through a one step method which combines the sol–gel chemistry and the spraying technique. Cheng *et al.*[232] reported the preparation of zirconia-based mesoporous materials with thermal stability up to 600 °C through post-treatment of the material synthesized from a zirconium sulfate precursor and a cationic CTAB surfactant.

Very recently, the hard-templating method has been introduced in the synthesis of mesoporous ZrO_2 as an important complement to the soft-templating method. Liu and Baker[233] employed SBA-15 as a hard template and $ZrOCl_2{\cdot}8H_2O$ as a precursor for the synthesis of ordered mesoporous ZrO_2 through the nanocasting process. However, a small amount of residual silicon remained in the zirconia framework due to the formation of Zr–O–Si bonds. The resultant ZrO_2 product exhibited a specific surface area of 220 $m^2\ g^{-1}$ and a pore volume of 0.57 $cm^3\ g^{-1}$. The pore size of 2.9 nm is a little larger than the wall thickness of SBA-15 (2.4 nm).

4.2.1.3 Hafnium oxide. Within the great group of mesoporous metal oxides, HfO_2 has been neglected for a long time, probably owing to the fact that there are also no prominent large scale applications of bulk hafnium oxide. However, it can be expected to show interesting physical properties both in the amorphous and crystalline states, and it could be useful for the preparation of strong acid catalysts. Sayari *et al.*[144] first reported the synthesis of thermally stable mesostructured HfO_2 with CTAB as a template. After removing the template at 500 °C, the obtained HfO_2 material showed a surface area of 204 $m^2\ g^{-1}$. Similar to many other metal oxides, HfO_2 with large mesopores can also be synthesized using a block copolymer as the template.[27,126]

4.2.2 V B group metal oxides

4.2.2.1 Vanadium oxide. Because the oxides and phosphates of vanadium are exceedingly important in catalysis, especially for the selective oxidation of hydrocarbons, considerable effort has been expended in synthesizing zeolites and simple oxides in which vanadium is substituted into the oxide framework. However, very few examples are reported for the preparation of mesoporous V_2O_5.[234] In most attempts only thermally unstable lamellar or hexagonal mesostructures have been produced.[235–237] The problem with V_2O_5 is its redox-instability, which makes soft-template removal rather difficult, and its solubility under alkaline and acidic conditions – and even in neutral water, which makes leaching of hard templates impossible without affecting the vanadia mesostructure.

4.2.2.2 Niobium oxide. Niobium oxide (Nb_2O_5) has been studied extensively due to its broad applications.[190] It is widely used in catalysis, as gas sensors, in electrochromic devices and in optical filters. Its variable oxidation states are useful to tailor catalytic properties and its acidic properties are relevant for acid-catalyzed reactions. Compared to vanadia, for niobium oxide it seems much easier to create the mesoporous oxides *via* a soft-templating method. Both amines[172,173,238,239] and block copolymers[27,29,128,133,174,175,190,240] are used as the templates. The space group of the mesostructures can be varied from lamellar,[172] over *p6mm*,[27,29,56,133,172–175] $P6_3/mmc$,[172,190] $Im\bar{3}m$,[128] and $Ia\bar{3}d$.[241] Ying and coworkers[172] first reported the synthesis of hexagonally packed mesoporous Nb_2O_5 with high stability (Fig. 12). The synthesis of this material was achieved through an approach using niobium(v) ethoxide $Nb(OEt)_5$ as a precursor, which can interact with the long chain of amines prior to condensation in the absence of water, thus obviating the use of acetylacetone and other chelating agents to control the condensation reaction. However, synthesis protocols using small-size surfactants have been superseded by the use of block copolymer templates after the first report by the Stucky group.[27] Using triblock copolymer P85 ($EO_{26}PO_{39}EO_{26}$) as a template, a highly ordered large pore 3-D mesostructured Nb_2O_5 with space group $P6_3/mmc$ can be synthesized.[190] In this case, a N^0I^0 route[23] with the addition of a trace amount of cations was used to fabricate the 3-D ordered mesostructure. By controlling the

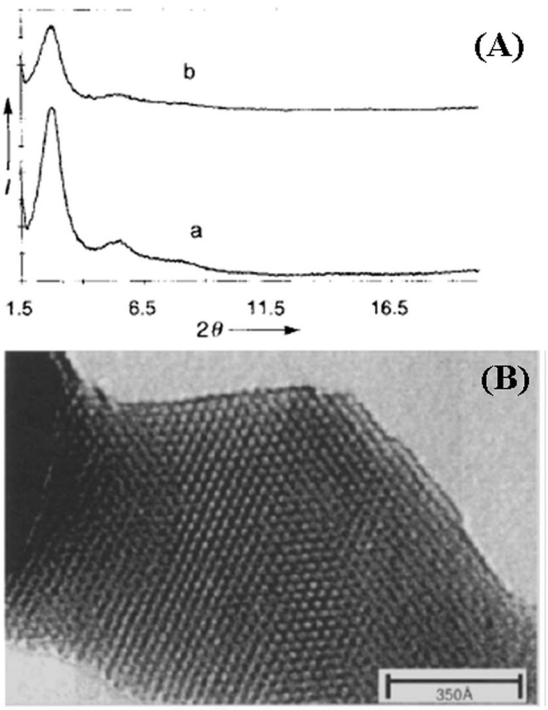

Fig. 12 XRD patterns (A) and TEM image (B) of mesoporous Nb_2O_5 synthesized with tetradecylamine as a structure directing agent. [Reprinted with permission from ref. 172, copyright 1996 Wiley.]

synthesis humidity, a 3-D cubic mesoporous niobium oxide with space group $Ia\bar{3}d$ can be synthesized with Pluronic P123 as a template *via* the EISA process.[241] After removal of the template, the pore wall of mesoporous niobium oxide is reinforced by carbon-filling. Crystalline niobium oxide with mesoporous structure can be obtained after crystallization at 600 °C in nitrogen, and subsequent carbon removal at 400 °C in oxygen.

4.2.2.3 Tantalum oxide. Tantalum oxide (Ta_2O_5) is useful in storage capacitors in large-scale integrated memory cells, and as a great insulator in metal oxide semiconductor (MOS) devices because of its high dielectric constant.[242] Mesoporous tantalum oxide was first synthesized by Antonelli and Ying through a ligand-assisted templating approach with long-chain primary amines.[181] The obtained material shows high hydrocarbon adsorption capacity which makes it a promising candidate as a catalyst support for hydrocarbon reforming. This kind of mesoporous Ta_2O_5 has also been used as a photocatalyst for water decomposition[243] and shape selective synthesis of linear alkyl benzenes.[182] Crystallization of the amorphous framework without losing the original ordered mesostructure can effectively enhance the photocatalytic activity for the total decomposition of water.[158] Recently, a 3-D cubic mesoporous Ta_2O_5 film with space group $Im\bar{3}m$ has been synthesized with diblock copolymers KLE as templates.[128] The mesoporous Ta_2O_5 film has iso-oriented layered nanocrystalline domains and possesses considerable potential as electrode material for electrochemical capacitor application.

4.2.3 VI B group metal oxides

4.2.3.1 Chromium oxide. Chromium oxides play an important role in magnetic recording, as pigments, and in catalysis.[244–246] For mesoporous chromium(III) oxide (Cr_2O_3), as for many other transition metal oxides, it is difficult to control the rate of precursor hydrolysis and condensation of the metal oxo species. Consequently, there are only few examples for the preparation of mesoporous chromium oxide with soft-templating methods.[188] Sinha *et al.*[188] used metal nitrate as a precursor, a nonaqueous mixture of ethylene glycol and propanol as solvent, and poly(alkylene oxide) block copolymer F127 as a template to prepare mesoporous chromium oxide with $Im\bar{3}m$ mesostructure. This mesoporous Cr_2O_3 material shows exceptionally high oxidation ability for volatile organic compounds (VOCs) (toluene, acetaldehyde). On the other hand, mesoporous silicas have been used as templates to successfully prepare mesoporous Cr_2O_3 with 2-D hexagonal $p6mm$ or 3-D cubic structures $Ia\bar{3}d$.[36,37,80] By using mesoporous silica KIT-6 as a template, a unique single-crystal Cr_2O_3 can be grown within the 3-D mesoporous system (Fig. 13).[80] This mesoporous Cr_2O_3 material shows greater capacity and better stability than its bulk counterpart for lithium-ion batteries.[247,248] In addition, ordered mesoporous Cr_2O_3 can be used as a catalyst to remove the VOCs such as toluene and ethyl acetate from air,[248,249] or used as a support for Keggin-type 12-phosphotungstic acids as an efficient catalyst for oxidation of benzyl alcohols.[250]

4.2.3.2 Molybdenum oxides. Molybdenum oxides have many potential applications such as in sensors, as catalysts, as photo-/electro-chromic materials, and in recording materials.[251–254] Antonelli *et al.*[255] first reported a mesostructured mixed oxidation state molybdenum oxide, which selectively formed toroidal shapes with a diameter of several hundred nanometers, using an as-synthesized dimeric molybdenum(V) ethoxide complex with a bridging dodecylimido group as a precursor. Using triblock copolymer micelles as templates, hollow MoO_3 nanospheres and porous network structure have been synthesized, but the network structure collapsed during the removal of the triblock copolymer. Lamellar molybdenum oxide-surfactant composite materials[256–259] were obtained by intercalating long chain quaternary ammonium surfactants into molybdic acid, MoO_3 powder, sodium molybdate or ammonium molybdate. However, the resulting mesoporous structures also collapsed upon removal of the template molecules. Using gemini surfactant as a template, lamellar mesoporous molybdenum(V/VI) oxide with retained structure after template removal was synthesized under mild conditions.[260,261] Highly ordered mesoporous molybdenum oxide with mixed valence and well-defined shapes was synthesized with PEO as a template.[193] The X-ray diffraction (XRD) pattern of the mesoporous molybdenum oxide shows more than 60 well-resolved reflection peaks, which can be indexed on the primitive cubic structure. This material has a BET surface area of 212 $m^2\ g^{-1}$, which is the highest one observed for mesoporous molybdenum oxide materials. The average mesopore diameter is 2.4 nm. Recently, Brezesinski *et al.*[127,128] used KLE as a template and synthesized an ordered mesoporous α-MoO_3 thin film with iso-oriented nanocrystalline

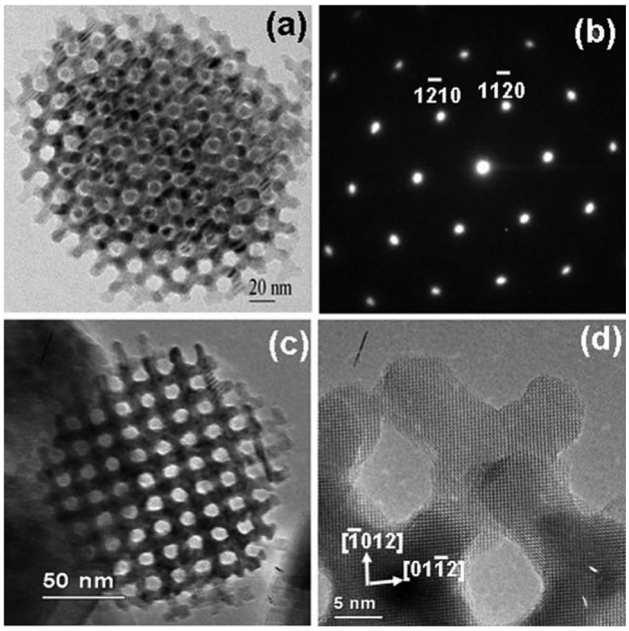

Fig. 13 TEM images of mesoporous single-crystal Cr_2O_3 templated by KIT-6 as a hard template. (a) TEM image viewed along the [111] direction. (b) The corresponding SAED pattern indexed onto the rhombohedral until cell of the Cr_2O_3 crystal. (c) TEM image viewed along the [100] direction. (d) The corresponding HRTEM image on the $[2\bar{2}1]$ zone axis of the Cr_2O_3 unit cell. [Reprinted with permission from ref. 80, copyright 2005 Royal Society of Chemistry.]

walls. This material shows a high electrochemical energy storage capacity.

4.2.3.3 Tungsten oxide. Tungsten oxide (WO_3) is an indirect bandgap semiconductor with interesting photoconductive behavior that has potential applications as a low cost material for solar energy devices.[262] Because of its distinct photochromic response and intercalation properties, it has also found use in electrochromic devices and chemical sensors.[263] In the early studies on the synthesis of mesoporous WO_3, low molecular weight surfactants were applied as soft templates. However, the obtained materials are thermally unstable.[23,196] Ordered mesoporous WO_3 can be synthesized by using a triblock copolymer as a template through the EISA method.[27,29] The obtained mesoporous WO_3 material has a *p6mm* mesostructure and a narrow pore size distribution centered at 5.0 nm.[27] Brezesinski *et al.*[131] used amphiphilic block copolymer KLE as a template for the synthesis of mesoporous WO_3 with a crystalline framework and $Im\bar{3}m$ mesostructure. The 3-D connected large mesopores (14 nm) facilitate the insertion of guest ions into the WO_3 network because of the shorter diffusion path lengths. The hard-templating method is another effective way for the preparation of ordered mesoporous WO_3; both SBA-15 and KIT-6 have been used as templates (Table 2).[264–269] Recently, Lee and coworkers synthesized a kind of ordered mesoporous WO_{3-x} with high conductivity, comparable to a mesoporous carbon framework, by using KIT-6 as a template. This material shows good performance as a catalyst for the oxygen reduction reaction (ORR)[267] and as a pseudocapacitor electrode.[268,269]

4.2.4 VII B group metal oxides. For group VII B elements, only manganese oxide has so far been obtained in mesoporous state. Manganese oxide has been widely used as a cathode material, catalyst, or magnetic material, owing to its outstanding structural flexibility, low cost of the raw materials, high specific capacitance, good electrochemical performance, and environmentally friendly nature. It is well known that the properties and performance of nanomaterials strongly depend on their phase, morphology and size. For example, electroactive materials with small crystalline particle sizes and controlled morphology usually show high electrochemical activities and excellent rate performance due to their high specific surface areas brought about by their interesting nanostructures. Therefore, many efforts have been invested in the preparation of manganese oxides with high surface area and controllable phase. Mesostructuring manganese oxides is one of the solutions to this problem. However, very few examples can be found for materials obtained by soft-templating.[142,171,270] Tian *et al.*[171] first prepared hexagonally and cubically structured mesoporous Mn_2O_3 and Mn_3O_4 by oxidation of $Mn(OH)_2$ in the presence of CTAB. These materials can be used as catalysts for the oxidation of cyclohexane and *n*-hexane in aqueous solutions.

The hard-templating method seems to be more versatile to synthesize ordered mesoporous manganese oxide with controllable mesostructure and crystalline phase. The Zhao group[37] used microwave-digested mesoporous SBA-15 as a template for the synthesis of mesoporous manganese oxide with a mixed crystal phase. Mesoporous manganese oxides with the β-MnO_2 phase have been synthesized by several groups.[271–275] Jiao *et al.*[272] used KIT-6 as a hard template to prepare mesoporous Mn_2O_3 by heating the Mn^{2+}-based precursor at 600 °C. Then the Mn_2O_3 phase was converted into the Mn_3O_4 phase by reducing it in 5% H_2 at 280 °C. Mesoporous manganese oxides show good performance in rechargeable lithium-ion batteries[271] and for catalytic decomposition of ammonium perchlorate.[275]

4.2.5 VIII group oxides

4.2.5.1 Iron oxides. Iron oxides are particularly important because of their applications in magnetic storage, as catalysts, and as electrodes for lithium-ion batteries. Many of these properties can be enhanced significantly when the materials are used in nanostructured form. Ordered mesoporous iron oxides with different valence states and structures have been prepared both by soft-[125,141,170,276] and hard-templating[37,78,277–281] methods. As observed for many other metal oxides, the soft-templating method mostly results in formation of disordered structures. Smarsly and coworkers[125] reported the synthesis of crack-free mesoporous α-Fe_2O_3 and α-FeOOH thin films, using the EISA method with diblock copolymer poly(isobutylene)-*block*-poly(ethylene oxide) (PIB-*b*-PEO) as a template. The diblock copolymer, featuring a high hydrophilic–hydrophobic contrast and relatively high thermal stability, is able to stabilize the mesostructured scaffold during conversion of the lattice structure from α-FeOOH into α-Fe_2O_3. Mesoporous silica SBA-15 and KIT-6 are also used as hard templates to fabricate ordered mesoporous iron oxides. Jiao *et al.* synthesized a series of ordered mesoporous iron oxides with different phases, including α-Fe_2O_3,[78] γ-Fe_2O_3,[278] and Fe_3O_4.[278] The Schüth group prepared mesoporous ferrihydrite by using the nanocasting route.[281,282]

4.2.5.2 Cobalt oxides. Cobalt oxide (Co_3O_4) is a technologically important material with applications in lithium-ion batteries,[283] gas sensors,[284] and electrochromic devices.[285] Nanostructured cobalt oxides with small crystal size and high surface area will show enhanced electrochemical activity and catalytic reactivity. In addition, cobalt oxide shows the best ordered mesostructures of all nanocast metal oxide materials. Various mesoporous silicas have been used as hard templates to fabricate ordered mesoporous Co_3O_4, including SBA-15[37,155,156,286–289] KIT-6,[155,156,286–288] SBA-16,[37,82] FDU-5,[79] vinylsilica,[153] and FDU-12.[82,290] Mesoporous Co_3O_4 nanowire arrays were first prepared by Tian and coworkers through the nanocasting method by using microwave digested SBA-15 and SBA-16 as hard templates.[35] The resultant porous materials have highly ordered mesostructures and copied as connected rods the topology of the SBA-15 pore system. Recently, ordered mesoporous CoO has been synthesized by reducing a mesostructured Co_3O_4 with glycerol, which had been prepared by nanocasting.[282,291] These nanocasted mesoporous cobalt oxide materials show high surface areas of up to 300 $m^2\ g^{-1}$ and have been used as catalysts[155,292] and as negative electrodes in rechargeable lithium-ion batteries.[288] The mesoporous structure also alters magnetic properties, thus solids with magnetic properties different from the bulk materials are obtained.[290,293–295] Very recently, a direct soft-templating

route was reported by Dahal *et al.*[296] In this case, Pluronic P123 was used as a template to synthesize highly ordered hexagonal mesoporous Co_3O_4 under well controlled conditions. The obtained cobalt oxide has a surface area as high as 367 $m^2\ g^{-1}$ and highly ordered hexagonal structure.

4.2.5.3 Nickel oxides. Nickel oxide (NiO) is a transition metal oxide semiconductor. It is a transparent, conducting, electrochromic and antiferromagnetic material, having a wide range of applications. It is a promising material for applications such as electro-chromic display devices, smart windows, active optical fibers, gas sensors, solar thermal absorbers, a catalyst for CO oxidation, fuel cell electrodes, and photoelectrolysis. The synthesis of ordered mesoporous nickel oxide using the surfactant SDS as a soft template was first reported by Banerjee *et al.*[176] The obtained nickel oxide shows a mesoporous structure with pore sizes ranging from 4 to 7 nm. Calcination at different temperatures was carried out, and the mesoporosity did not collapse even after calcination at 500 °C, although the surface area decreased strongly (from 279 to 72 $m^2\ g^{-1}$) and a broadening of the pore size distribution was observed. This mesoporous NiO shows good capacitive behavior due to its unique mesoporous structure.[145] If mesoporous silicas are used as hard templates, ordered mesoporous NiO with space groups *p6mm*,[37,297] $Im\bar{3}m$,[82] $Fm\bar{3}m$,[82] and $Ia\bar{3}d$[154] can be obtained. Jiao and Bruce reported the synthesis of mesoporous NiO with crystalline walls and an ordered pore structure, exhibiting a bimodal pore size distribution (3.3 and 11 nm), by using KIT-6 as a template. By controlling the micropores connecting the two sets of mesopore systems in the KIT-6 template, the relative proportions of the two pore sizes can be adjusted.

4.2.5.4 Ruthenium oxide. Ruthenium oxide (RuO_2) is one of the most promising electrode materials for supercapacitor applications. Mesoporous ruthenium oxide is seldom reported in the literature. Anhydrous disordered mesoporous ruthenium oxide was synthesized by a simple non-ionic surfactant templating method using Pluronic P123, and tested as an active electrode material for an electrochemical supercapacitor.[298] The capacitance for anhydrous RuO_2 was found to be 58 $F\ g^{-1}$. RuO_2-based mesoporous thin films of optical quality were synthesized from ruthenium-peroxo-based sols using micelle templates made of amphiphilic PS-*b*-PEO block copolymers.[135] This mesoporous RuO_2 material exhibits capacitances as high as 1000 ± 100 $F\ g^{-1}$ at a scan rate of 10 $mV\ s^{-1}$. Besides the soft-templating method, highly ordered mesoporous RuO_2 has also been successfully synthesized *via* the nanocasting method by controlling the surface hydrophobicity of KIT-6.[299] The obtained mesoporous RuO_2 material with well-defined mesostructure and high surface area (131 $m^2\ g^{-1}$) exhibited excellent catalytic activity for CO oxidation.

4.2.6 I B group metal oxides. Among group I B elements, only copper is normally obtained as oxide instead of the neat metal. Copper-based oxides are well known components of catalysts and are widely employed commercially for the direct N_2O decomposition, CO oxidation, and the complete combustion of hydrocarbons.[300–302] Mesoporous copper oxides with an ordered pore structure, high specific surface area, and crystalline walls are expected to provide enhanced catalytic performance in the above-mentioned reactions since they can be regarded as self-supported catalysts with a high activity due to their high specific surface area and a certain degree of size and shape selectivity. However, only a few cases can be discussed here due to the low stability of the products. A Cu_2O film has been prepared on ITO(Sn-doped In_2O_3)-covered glass substrates by electrochemical deposition from lyotropic liquid crystalline phases with the polyoxyethylene surfactant Brij 76 ($C_{18}EO_{10}$).[303] However, the authors did not mention the removal of the template, and one might suspect that the film structure would collapse upon such attempts. Recently, Shang *et al.*[304] prepared mesoporous Cu_2O spheres with short-range-ordered mesostructures by using Pluronic P123 as a structure directing agent. Lai *et al.*[84] prepared a highly ordered mesoporous copper oxide with uniform SBA-15-like mesostructure using CMK-3 as a hard template. However, the study lacks high resolution TEM evidence, and sharp high angle XRD peaks are not well explained, so that possibly a phase mixture was obtained in this case.

4.2.7 II B group metal oxides. It is only zinc oxide (ZnO) that has been studied in this group. Zinc oxide is attracting tremendous research interest due to its vast spectrum of properties and applications. ZnO is an n-type semiconductor with a band-gap of 3.37 eV. It has piezoelectric- and electromechanical-coupling properties. It can be used in diodes, lasers, photovoltaic solar cells, and gas sensors. In addition, ZnO is one of the important components in industrial methanol-synthesis catalysts. The creation of ZnO with high surface area could enhance the activity in catalysis. With soft-templating methods, only disordered mesoporous ZnO materials can be synthesized.[305,306] Mesoporous zinc oxide with a wurtzite-like nanocrystalline framework has been synthesized by using Schiff-base amine as a template. The resulting material shows a very high BET surface area of 456 $m^2\ g^{-1}$ and remarkably enhanced photoconductivity and photoluminescence at room temperature under visible light irradiation.[306] By using mesoporous carbon as a hard template, ordered mesoporous ZnO can be obtained with high surface area.[307–310] Polarz *et al.*[307] reported the synthesis of ordered mesoporous ZnO by using a special liquid phase organometallic $\{(CH_3ZnOR)_4\}$ as a precursor and ordered mesoporous CMK-3 as a hard template. The organometallic functionalities (Zn–CH_3) of the precursors are very important because they enable the preparation of ZnO in nanocrystalline form, either thermolytically at low temperatures, or hydrolytically. Recently, Grosso and coworkers[311] reported the synthesis of mesoporous ZnO films *via* a hard-templating method by using mesoporous silica as a template. It had been argued that ZnO cannot be prepared with silica as a hard template, because ZnO would not only react with base solution, but also react with HF, so that a silica template could not be selectively etched. However, in this case the silica template was removed by carefully adjusting the pH value of the KOH solution and the leaching time. At pH values around 12, amorphous silica is around 1000 times more soluble than ZnO, leading to selective removal of silica, but not of ZnO.

4.3 Rare earth oxides

Rare earth oxides and mixed oxides are useful as materials with luminescent, electric, catalytic, and magnetic properties that result from their 4f electrons. Rare earth garnets are applicable as bubble memory materials owing to their small magnetic domains with up or down spins. If such rare earth oxides were obtainable as mesoporous solids, they would be promising as adsorbents or separating agents with a combination of shape- or size-selectivity and magnetic properties. They could also act as electrically, magnetically, or optically functional host materials. However, up to now not much attention has been paid to this area. In early attempts only some mesostructured materials with thermally unstable frameworks were obtained.[312] Yada *et al.*[117] used SDS as a template to synthesize a series of ordered mesoporous rare earth oxides, including the elements Gd, Tb, Dy, Ho, Er, Tm, Yb, and Lu. The surfactant was removed by anion exchange with acetate ions. High surface areas of 257–348 $m^2 g^{-1}$ have been obtained for these rare earth oxides. Morris and coworkers[118] used the neutral surfactant hexadecylamine as a template for the synthesis of mesoporous rare earth oxides with the framework containing La, Pr, Nd, Sm, Gd, Er, and Yb. Castro *et al.*[132] synthesized mesoporous Y_2O_3 with KLE as a template. Lundberg *et al.* prepared mesoporous CeO_2 with Pluronic P123. The obtained materials show high BET surface area (up to 150 $m^2 g^{-1}$), but have disordered mesostructure.[313] Laberty-Robert and Sanchez recently prepared ceria and cermet NiO/Gd-doped ceria mesoporous thin films by using block copolymer PS-*b*-PEO as a soft template, and integrated these as anodes for solid oxide fuel cell (SOFC).[314–316]

Also the nanocasting method has been used to fabricate mesoporous rare earth oxides. Ryoo and coworkers[317] first reported the synthesis of mesoporous CeO_2 with SBA-15 and KIT-6 as hard templates. The obtained materials have highly ordered mesostructures and nanocrystalline pore walls, and exhibit high thermal stability up to 700 °C. Shi and coworkers[318] used this kind of CeO_2 as CuO support for catalytic CO oxidation. Tiemann and coworkers[319] used mesoporous carbon CMK-3 as a template for the synthesis of mesoporous CeO_2 and used the resulting material as a catalyst for methanol decomposition. More recently, a novel metal–organic framework (MOF)-driven approach was used to prepare hierarchical mesoporous CeO_2 and MgO with nanopores and high specific surface area.[320]

4.4 Alkaline earth oxides

Alkaline earth oxides have a wide range of applications in adsorption, microelectronics, and catalysis.[321] Due to their strong basic properties, alkaline earth oxides can be used as adsorbents for acidic gases such as SO_2 and CO_2. MgO and CaO are the most often investigated alkaline earth oxides. CaO is a catalyst component for oxidative dehydrogenation and isomerization of alkenes. MgO shows strongly basic properties that can be exploited for base catalysis in many organic reactions, such as alcohol dehydrogenation. Dai and coworkers[322] synthesized 3-D mesoporous single-crystalline CaO nano- and microparticles with tri-, tetra-, and hexagonal morphologies with Pluronic P123,

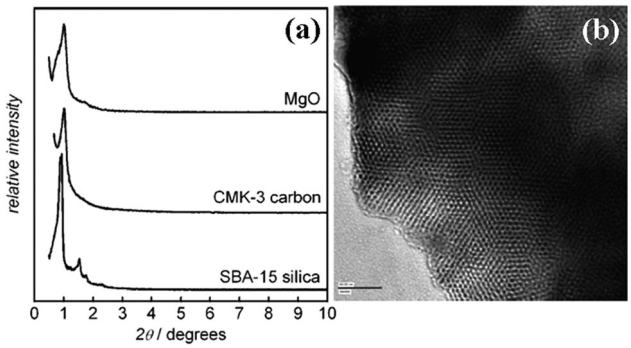

Fig. 14 (a) Powder X-ray diffraction diagrams of mesoporous magnesium oxide and CMK-3 carbon/SBA-15 silica templates; (b) TEM image of mesoporous magnesium oxide templated by CMK-3. [Reprinted with permission from ref. 77, copyright 2005 American Chemical Society.]

CTAB, or PEG (polyethylene glycol) as auxiliaries. With the same concept, they also synthesized MgO with hierarchical mesoporous and macroporous porosity.[323] However, the mesostructures are disordered. More recently, Eckhardt *et al.*[324] reported the synthesis of mesoporous $MgCO_3$ and MgO films with PEO–PB–PEO as a template. For the hard-templating method, mesoporous carbon can also be used to fabricate alkaline earth oxides. Li *et al.*[325] used mesoporous carbon aerogel as a hard template and magnesium nitrate solution as a MgO precursor to synthesize mesoporous – albeit disordered – MgO with high surface area up to 150 $m^2 g^{-1}$. Tiemann and coworkers[77] used mesoporous carbon CMK-3 as a template to successfully synthesize highly ordered mesoporous MgO with surface areas as high as 306 $m^2 g^{-1}$ (Fig. 14). This kind of material has been used as a base catalyst in the Baeyer–Villiger oxidation of cyclic ketones to the corresponding lactones. 100% adamantanone conversion and >99% lactone selectivity were obtained over mesoporous MgO materials.[326]

4.5 Complex metal oxides (spinel structure)

Complex metal oxides with spinel structure are of intense interest due to their remarkable optical, electrical, magnetic, and catalytic properties, having potential applications in areas such as magnetic storage, magnetic resonance imaging, catalysis, and rechargeable lithium-ion batteries.[327,328] The particle size, morphology and porosity are recognized as important factors which have significant influence on the structural, physical and chemical properties of spinels.[329] Mesoporous spinel oxides with high surface area and uniform pore diameters are desirable especially for processes taking place at the phase boundary between solid particles and a liquid or gas phase as well as those relying on the flux of molecules or ions to and from active surfaces. However, it is still a challenge to synthesize ordered mesoporous spinel-type complex metal oxides by the soft-templating method.[330–333] In contrast, there are numerous reports on the synthesis of these oxides by nanocasting.[334–340]

Carreon *et al.*[332] reported the synthesis of mesoporous nanocrystalline cobalt nickel oxide spinels by self-assembly of heterometallic alkoxides in the presence of supramolecular

liquid crystalline phases. The resultant mesoporous cobalt nickel oxides exhibited higher propane conversion to CO and CO_2 as compared to a conventional dense spinel. Nevertheless it is not a trivial task to extend this soft-chemistry approach to prepare other simple or complex oxides, because the hydrolysis and condensation of transition-metal alkoxides (if available at all) are difficult to control precisely; as a result, the obtained metal oxides are susceptible to be phase separated and usually show poor structural ordering and low thermal stability after removal of the surfactant templates.[9] Mesoporous $CoFe_2O_4$ that exhibits tunable room temperature ferromagnetism has been fabricated by co-assembly of inorganic precursors with a large amphiphilic diblock copolymer, referred to as KLE.[341] The inverse spinel framework is formed with an ordered open network of pores averaging 14 nm in diameter. The domain sizes of the crystallites are tunable from 6 to 15 nm.

As an alternative, the hard-templating route successfully overcomes the aforementioned problem of structural instability encountered by the soft-templating approach. Furthermore, hard templates with topologically stable frameworks could sustain the local strain caused by crystallization of the precursors; it is thus expected to prepare mesoporous metal oxides with crystalline walls which could provide superior properties (*e.g.* mechanical and thermal stability) necessary for practical applications. In addition, multicomponent metal oxides should be more easily fabricated *via* this hard-template route, since *via* the solution based precursors one could effectively control the homogeneity and stoichiometry of the resultant replicas. Numerous complex metal oxides have been synthesized *via* the nanocasting method. Valdés-Solís and coworkers[335] used mesoporous silica xerogel as a hard template and synthesized high surface area $CuCr_2O_4$, $CuMn_2O_4$ and $NiMn_2O_4$ complex spinel oxides. Mesoporous, although disordered, $MgAl_2O_4$ spinel monoliths were synthesized by the nanocasting pathway with a carbon aerogel monolith as a template.[334] Au-catalysts based on this spinel material as a support show high activity in CO oxidation. Well ordered mesoporous spinel-structured $LiMn_2O_4$ was prepared by the chemical lithiation of mesoporous MnO_2 and the resulting material was used as cathode material for lithium-ion batteries.[342] With a similar process, Jiao *et al.*[336] also prepared a 3-D mesoporous $Li_{1.12}Mn_{1.88}O_4$ with enhanced capacity compared to bulk materials. Nanocrystalline mesoporous $ZnAl_2O_4$ thin films have been synthesized by using the soft-templating method with Pluronic F127 as a template through the EISA process.[333] He and coworkers[337] synthesized mesoporous $NiFe_2O_4$, $MgFe_2O_4$ and $CoFe_2O_4$ with SBA-15 as a template *via* a two-solvent method. Mesoporous spinels ($CuCo_2O_4$, $MnCo_2O_4$ and $NiCo_2O_4$) with crystalline frameworks have been synthesized through a nanocasting pathway using concentrated solutions of metal nitrates as precursors and mesoporous silica SBA-15 as the hard template.[338] The $CuCo_2O_4$ and $MnCo_2O_4$ catalysts exhibit high activities and robust stabilities in CO oxidation. Mesoporous $CoFe_2O_4$ with both *p6mm* and $Ia\bar{3}d$ structures was discussed in detail by Ji and coworkers.[339] Magnetic tests showed that both samples have rather low coercivity (106.5 and 212.1 Oe, respectively) due to the presence of a prominent proportion of superparamagnetic particles. Highly ordered mesoporous $NiFe_2O_4$ with excellent microwave absorption properties has been synthesized by using mesoporous silica (KIT-6) as a hard template.[340]

4.6 Others

Beyond the above mentioned metal oxides, many other metal oxides are also synthesized (Tables 1 and 2). Discussing all of these in detail would exceed the scope of this review and we have thus focused on the more interesting systems from an applications point of view, or on such that are prototypic for specific synthetic pathways. However, some of the other systems shall at least briefly be addressed. High surface area mesoporous Ga_2O_3 can be synthesized using soft-templating methods, but the structures are disordered.[143,343,344] In_2O_3 with various mesostructures have been prepared with mesoporous silica[37,79,82,161,345–347] or carbon[348] as templates. Mesostructured GeO_2 can be fabricated with surfactants as structure directing agents, but the templates cannot be removed effectively.[349,350] Zou *et al.*[351] prepared a mesoporous GeO_2 with gyroidal channels, separated by crystalline walls by a hydrothermal method. The pore size of this crystalline GeO_2 reached 1.2 nm, and the surface area was as high as 214 $m^2 g^{-1}$. Mesoporous SnO_2 materials have been prepared both using a surfactant and mesoporous silica as a template.[27,29,113,129,178–180,352,353] They have potential applications in gas sensors[179,180,354] and batteries.[353] By using diblock copolymer KLE as a template, mesoporous Bi_2O_3 films with cubic structure have also been prepared.[123]

Mesoporous multimetal oxides beyond spinel structure, such as perovskite oxides, also have been prepared.[330,355–362] Perovskite oxides are important materials with applications that range from catalysis, oxygen membranes, to magnetism, and others. Perovskite structures are complex mixed metal oxide phases which can contain almost any element of the periodic table. The fact that they have been accommodated in the mesoporous world is another sign that the synthesis of mesoporous materials can probably be extended to any kind of structure.

5. Summary and outlook

Ordered mesoporous metal oxides have attracted high interest due to their diverse – and often unique – properties, functionalities and potential applications, as compared to their silica counterparts. Substantial achievements have been made with respect to synthesis and structural characterization, especially in the last ten years. As of now, most of the elements of the periodic table can be used as basis for mesoporous frameworks, using various methods. Recent breakthroughs in the synthetic methods of mesoporous metal oxides have opened up a new field of porous materials research, making the applications of mesoporous materials in the fields of catalysis, sensing, and electrochemistry possible. High molecular weight block copolymers become more and more common soft templates for the preparation of ordered mesoporous metal oxides with large pores. Nanocasting methods can be used to synthesize most of

the metal oxides which cannot easily be prepared by soft-templating methods. Their negative replica mesostructures and smaller particle sizes allow easy gas transfer in their pore systems. Furthermore, the crystalline framework of the nanocast metal oxides can be an advantage in many applications as opposed to the amorphous porous silicas. The cost of production of ordered mesoporous metal oxides is certainly an obstacle for their widespread application. However, as compared to the silicas, the relative cost disadvantage of mesoporous materials over bulk materials is lower, since the raw material costs of metal oxides are often substantially higher than for silica. This reduces the relative cost fraction incurred by the templates, possibly lowering the threshold for applications compared to silica.

This review has tried to summarize the state of the art in the synthesis of ordered mesoporous metal oxides. Due to the great variety of materials and synthetic conditions, it is almost impossible to be fully comprehensive. However, we have tried to discuss in some more detail both the prototypical examples for specific methods, and the materials for which there seems to be a high level of current research interest. With the information given in this review, the reader should be able to find the information on the synthesis and properties of specific materials, and to find guidance for the production of hitherto unaccessible metal oxide compositions or phases.

However, although great progress in the synthesis of the mesoporous metal oxides has been made, a simple, facile and general method for their production is still lacking. For each composition and phase, the protocols have to be meticulously established, and formation of specific compounds is often highly sensitive to conditions. For example, some surfactants are successful for the synthesis of specific metal oxides but not suitable for others. The nanocasting method can result in crystalline frameworks, but it is difficult to adjust the pore sizes. Production of high quality mesoporous metal oxides with uniform nanostructures is still a great challenge for most oxides. Especially challenging is the synthesis of single crystalline mesoporous oxides. Some metal oxides can be synthesized in a form, in which each mesoporous particle is a single crystal penetrated by the pores, without grain boundaries inside the pore walls. This kind of material is expected to have interesting properties, especially when the orientation of the crystal lattice and the mesostructure pattern can be well controlled.[102]

Practical applications, on the other hand, are far behind the synthesis of ordered mesoporous metal oxides. This is not only due to the high price of the template and the special precursors for producing mesoporous metal oxides, but also to difficulties in controlling the quality when it comes to mass production. While the scale-up problem is little explored, it can be expected that substantial obstacles will have to be passed before large scale production is guaranteed and reproducible quality is possible. Problems are expected at the stage of mesostructure formation itself on the larger scale, if solution based processes are employed with much more substantial mixing problems, or in the case of hard-templating, in the crucial impregnation step which is difficult to scale up. Also the template removal will not be straightforward, since in deeper beds of material gradients are more difficult to control. For large scale production, probably continuous processes, such as spray synthesis, are most suitable, since the scale remains locally relatively small at the mesophase formation stage, but large amounts are accessible over longer operation times, or parallelization of setups.

Exploring applications beyond mere proof-of-concept studies is one of the most important issues in this area, and such applications may lie in fields such as catalysis, energy storage, solar cells or sensors. As stated above, the relative cost disadvantage is lower – compared to silica – for many ordered mesoporous metal oxides, and thus more attention from both the academic and industrial research community should be focused on this class of materials. New synthetic strategies, which can reduce prices and can be easily scaled up without losing quality, need to be developed. More efforts should also be devoted to the study of the properties of the novel mesoporous oxides family which go beyond the mere structural and textural characterization, but are focused on properties, such as electronic or magnetic features in order to explore unconventional application fields.

However, to some extent we are confronted with a hen-and-egg problem: currently, high quality ordered mesoporous materials can only be produced by a limited number of groups typically on a small scale, and there is no commercial source for scientists or companies who would like to test the materials in specific applications, so that many potential applications may not be explored. On the other hand, as long as there is no big market for ordered mesoporous oxides, no company would invest in scale-up of the production routes in order to supply commercial materials. Here might be an opportunity for small specialty manufacturers who could produce and offer desired materials on demand only.

However, one should consider that also ordered mesoporous silicas, the development of which is five to ten years ahead of that of non-silica metal oxides, are not yet widely applied, and thus probably some patience is required. The novel concepts for the synthesis of solids developed in this field will certainly be of lasting value, even if no applications will arise in the near future.

Acknowledgements

We thank Wei Li for his assistance in preparing the review. We greatly acknowledge the support of this research by the Alexander von Humboldt-Stiftung, in addition to the basic support by the Max-Plank-Society.

References

1 T. Yanagisawa, T. Shimizu, K. Kuroda and C. Kato, *Bull. Chem. Soc. Jpn.*, 1990, **63**, 988.
2 C. T. Kresge, M. E. Leonowicz, W. J. Roth, J. C. Vartuli and J. S. Beck, *Nature*, 1992, **359**, 710.
3 J. S. Beck, J. C. Vartuli, W. J. Roth, M. E. Leonowicz, C. T. Kresge, K. D. Schmitt, C. T. W. Chu, D. H. Olson, E. W. Sheppard, S. B. McCullen, J. B. Higgins and J. L. Schlenker, *J. Am. Chem. Soc.*, 1992, **114**, 10834.

4 Y. Ren, Z. Ma and P. G. Bruce, *Chem. Soc. Rev.*, 2012, **41**, 4909.
5 A. Corma, *Chem. Rev.*, 1997, **97**, 2373.
6 K. Moller and T. Bein, *Chem. Mater.*, 1998, **10**, 2950.
7 U. Ciesla and F. Schüth, *Microporous Mesoporous Mater.*, 1999, **27**, 131.
8 J. Y. Ying, C. P. Mehnert and M. S. Wong, *Angew. Chem., Int. Ed.*, 1999, **38**, 56.
9 F. Schüth, *Chem. Mater.*, 2001, **13**, 3184.
10 M. E. Davis, *Nature*, 2002, **417**, 813.
11 F. Schüth and W. Schmidt, *Adv. Mater.*, 2002, **14**, 629.
12 G. J. D. Soler-illia, C. Sanchez, B. Lebeau and J. Patarin, *Chem. Rev.*, 2002, **102**, 4093.
13 F. Schüth, *Angew. Chem., Int. Ed.*, 2003, **42**, 3604.
14 M. Hartmann, *Chem. Mater.*, 2005, **17**, 4577.
15 A. Taguchi and F. Schüth, *Microporous Mesoporous Mater.*, 2005, **77**, 1.
16 A. H. Lu and F. Schüth, *Adv. Mater.*, 2006, **18**, 1793.
17 M. Vallet-Regi, F. Balas and D. Arcos, *Angew. Chem., Int. Ed.*, 2007, **46**, 7548.
18 Y. Wan and D. Y. Zhao, *Chem. Rev.*, 2007, **107**, 2821.
19 C. D. Liang, Z. J. Li and S. Dai, *Angew. Chem., Int. Ed.*, 2008, **47**, 3696.
20 Y. F. Shi, Y. Wan and D. Y. Zhao, *Chem. Soc. Rev.*, 2011, **40**, 3854.
21 H. Tüysüz and F. Schüth, *Adv. Catal.*, 2012, **55**, 127.
22 A. Monnier, F. Schüth, Q. Huo, D. Kumar, D. Margolese, R. S. Maxwell, G. D. Stucky, M. Krishnamurty, P. Petroff, A. Firouzi, M. Janicke and B. F. Chmelka, *Science*, 1993, **261**, 1299.
23 Q. S. Huo, D. I. Margolese, U. Ciesla, P. Y. Feng, T. E. Gier, P. Sieger, R. Leon, P. M. Petroff, F. Schüth and G. D. Stucky, *Nature*, 1994, **368**, 317.
24 D. M. Antonelli and J. Y. Ying, *Angew. Chem., Int. Ed. Engl.*, 1995, **34**, 2014.
25 Y. F. Lu, R. Ganguli, C. A. Drewien, M. T. Anderson, C. J. Brinker, W. L. Gong, Y. X. Guo, H. Soyez, B. Dunn, M. H. Huang and J. I. Zink, *Nature*, 1997, **389**, 364.
26 R. Ryoo, S. H. Joo and S. Jun, *J. Phys. Chem. B*, 1999, **103**, 7743.
27 P. D. Yang, D. Y. Zhao, D. I. Margolese, B. F. Chmelka and G. D. Stucky, *Nature*, 1998, **396**, 152.
28 P. D. Yang, T. Deng, D. Y. Zhao, P. Y. Feng, D. Pine, B. F. Chmelka, G. M. Whitesides and G. D. Stucky, *Science*, 1998, **282**, 2244.
29 P. D. Yang, D. Y. Zhao, D. I. Margolese, B. F. Chmelka and G. D. Stucky, *Chem. Mater.*, 1999, **11**, 2813.
30 Y. Meng, D. Gu, F. Q. Zhang, Y. F. Shi, H. F. Yang, Z. Li, C. Z. Yu, B. Tu and D. Y. Zhao, *Angew. Chem., Int. Ed.*, 2005, **44**, 7053.
31 F. Q. Zhang, Y. Meng, D. Gu, Y. Yan, C. Z. Yu, B. Tu and D. Y. Zhao, *J. Am. Chem. Soc.*, 2005, **127**, 13508.
32 D. Gu, H. Bongard, Y. H. Deng, D. Feng, Z. X. Wu, Y. Fang, J. J. Mao, B. Tu, F. Schüth and D. Y. Zhao, *Adv. Mater.*, 2010, **22**, 833.
33 D. Gu, H. Bongard, Y. Meng, K. Miyasaka, O. Terasaki, F. Q. Zhang, Y. H. Deng, Z. X. Wu, D. Feng, Y. Fang, B. Tu, F. Schüth and D. Y. Zhao, *Chem. Mater.*, 2010, **22**, 4828.
34 S. H. Joo, S. J. Choi, I. Oh, J. Kwak, Z. Liu, O. Terasaki and R. Ryoo, *Nature*, 2001, **412**, 169.
35 Z. Liu, Y. Sakamoto, T. Ohsuna, K. Hiraga, O. Terasaki, C. H. Ko, H. J. Shin and R. Ryoo, *Angew. Chem., Int. Ed.*, 2000, **39**, 3107.
36 K. K. Zhu, B. Yue, W. Z. Zhou and H. Y. He, *Chem. Commun.*, 2003, 98.
37 B. Z. Tian, X. Y. Liu, H. F. Yang, S. H. Xie, C. Z. Yu, B. Tu and D. Y. Zhao, *Adv. Mater.*, 2003, **15**, 1370.
38 D. Y. Zhao, Z. H. Luan and L. Kevan, *Chem. Commun.*, 1997, 1009.
39 T. Kimura, Y. Sugahara and K. Kuroda, *Chem. Mater.*, 1999, **11**, 508.
40 B. Z. Tian, X. Y. Liu, B. Tu, C. Z. Yu, J. Fan, L. M. Wang, S. H. Xie, G. D. Stucky and D. Y. Zhao, *Nat. Mater.*, 2003, **2**, 159.
41 J. Y. Kim, S. B. Yoon, F. Kooli and J. S. Yu, *J. Mater. Chem.*, 2001, **11**, 2912.
42 F. Gao, Q. Y. Lu and D. Y. Zhao, *Adv. Mater.*, 2003, **15**, 739.
43 Y. F. Shi, Y. Wan, R. L. Liu, B. Tu and D. Y. Zhao, *J. Am. Chem. Soc.*, 2007, **129**, 9522.
44 P. Dibandjo, F. Chassagneux, L. Bois, C. Sigala and P. Miele, *J. Mater. Chem.*, 2005, **15**, 1917.
45 Y. F. Shi, Y. Meng, D. H. Chen, S. J. Cheng, P. Chen, T. F. Yang, Y. Wan and D. Y. Zhao, *Adv. Funct. Mater.*, 2006, **16**, 561.
46 Y. F. Shi, Y. Wan, R. Y. Zhang and D. Y. Zhao, *Adv. Funct. Mater.*, 2008, **18**, 2436.
47 Z. L. Yang, Y. F. Lu and Z. Z. Yang, *Chem. Commun.*, 2009, 2270.
48 C. Sanchez, C. Boissière, D. Grosso, C. Laberty and L. Nicole, *Chem. Mater.*, 2008, **20**, 682.
49 D. Grosso, F. Cagnol, G. Soler-Illia, E. L. Crepaldi, H. Amenitsch, A. Brunet-Bruneau, A. Bourgeois and C. Sanchez, *Adv. Funct. Mater.*, 2004, **14**, 309.
50 D. Grosso, G. Soler-Illia, F. Babonneau, C. Sanchez, P. A. Albouy, A. Brunet-Bruneau and A. R. Balkenende, *Adv. Mater.*, 2001, **13**, 1085.
51 E. L. Crepaldi, D. Grosso, G. Soler-Illia, P. A. Albouy, H. Amenitseh and C. Sanchez, *Chem. Mater.*, 2002, **14**, 3316.
52 G. Soler-Illia, A. Louis and C. Sanchez, *Chem. Mater.*, 2002, **14**, 750.
53 E. L. Crepaldi, G. Soler-Illia, A. Bouchara, D. Grosso, D. Durand and C. Sanchez, *Angew. Chem., Int. Ed.*, 2003, **42**, 347.
54 E. L. Crepaldi, G. Soler-Illia, D. Grosso, F. Cagnol, F. Ribot and C. Sanchez, *J. Am. Chem. Soc.*, 2003, **125**, 9770.
55 D. Grosso, G. Soler-Illia, E. L. Crepaldi, F. Cagnol, C. Sinturel, A. Bourgeois, A. Brunet-Bruneau, H. Amenitsch, P. A. Albouy and C. Sanchez, *Chem. Mater.*, 2003, **15**, 4562.
56 J. Fan, S. W. Boettcher and G. D. Stucky, *Chem. Mater.*, 2006, **18**, 6391.
57 Y. F. Lu, H. Y. Fan, A. Stump, T. L. Ward, T. Rieker and C. J. Brinker, *Nature*, 1999, **398**, 223.

58 C. Boissière, D. Grosso, A. Chaumonnot, L. Nicole and C. Sanchez, *Adv. Mater.*, 2011, **23**, 599.
59 C. Boissière, D. Grosso, H. Amenitsch, A. Gibaud, A. Coupe, N. Baccile and C. Sanchez, *Chem. Commun.*, 2003, 2798.
60 C. K. Tsung, J. Fan, N. F. Zheng, Q. H. Shi, A. J. Forman, J. F. Wang and G. D. Stucky, *Angew. Chem., Int. Ed.*, 2008, **47**, 8682.
61 C. Boissière, L. Nicole, C. Gervais, F. Babonneau, M. Antonietti, H. Amenitsch, C. Sanchez and D. Grosso, *Chem. Mater.*, 2006, **18**, 5238.
62 J. H. Kim, K. Y. Jung, K. Y. Park and S. B. Cho, *Microporous Mesoporous Mater.*, 2010, **128**, 85.
63 D. A. Konopka, S. Pylypenko, P. Atanassov and T. L. Ward, *ACS Appl. Mater. Interfaces*, 2010, **2**, 86.
64 H. F. Yang and D. Y. Zhao, *J. Mater. Chem.*, 2005, **15**, 1217.
65 C. R. Martin, *Science*, 1994, **266**, 1961.
66 C. M. Zelenski and P. K. Dorhout, *J. Am. Chem. Soc.*, 1998, **120**, 734.
67 A. H. Lu and F. Schüth, *C. R. Chim.*, 2005, **8**, 609.
68 C. Z. Yu, J. Fan, B. Z. Tian, D. Y. Zhao and G. D. Stucky, *Adv. Mater.*, 2002, **14**, 1742.
69 T. W. Kim, R. Ryoo, K. P. Gierszal, M. Jaroniec, L. A. Solovyov, Y. Sakamoto and O. Terasaki, *J. Mater. Chem.*, 2005, **15**, 1560.
70 B. Z. Tian, S. A. Che, Z. Liu, X. Y. Liu, W. B. Fan, T. Tatsumi, O. Terasaki and D. Y. Zhao, *Chem. Commun.*, 2003, 2726.
71 A. H. Lu, W. Schmidt, A. Taguchi, B. Spliethoff, B. Tesche and F. Schüth, *Angew. Chem., Int. Ed.*, 2002, **41**, 3489.
72 M. Kang, S. H. Yi, H. I. Lee, J. E. Yie and J. M. Kim, *Chem. Commun.*, 2002, 1944.
73 A. Sakithivel, S. Huang, W. Chen, T. Kim, R. Ryoo, A. S. T. Chiang, K. Chen and S. B. Liu, *Stud. Surf. Sci. Catal.*, 2004, **154**, 394.
74 A. H. Lu, W. Schmidt, B. Spliethoff and F. Schüth, *Chem.–Eur. J.*, 2004, **10**, 6085.
75 A. Sakthivel, S. J. Huang, W. H. Chen, Z. H. Lan, K. H. Chen, T. W. Kim, R. Ryoo, A. S. T. Chiang and S. B. Liu, *Chem. Mater.*, 2004, **16**, 3168.
76 P. Dibandjo, L. Bois, F. Chassagneux, D. Cornu, J. M. Letoffe, B. Toury, F. Babonneau and P. Miele, *Adv. Mater.*, 2005, **17**, 571.
77 J. Roggenbuck and M. Tiemann, *J. Am. Chem. Soc.*, 2005, **127**, 1096.
78 F. Jiao, A. Harrison, J. C. Jumas, A. V. Chadwick, W. Kockelmann and P. G. Bruce, *J. Am. Chem. Soc.*, 2006, **128**, 5468.
79 B. Z. Tian, X. Y. Liu, L. A. Solovyov, Z. Liu, H. F. Yang, Z. D. Zhang, S. H. Xie, F. Q. Zhang, B. Tu, C. Z. Yu, O. Terasaki and D. Y. Zhao, *J. Am. Chem. Soc.*, 2004, **126**, 865.
80 K. Jiao, B. Zhang, B. Yue, Y. Ren, S. X. Liu, S. R. Yan, C. Dickinson, W. Z. Zhou and H. Y. He, *Chem. Commun.*, 2005, 5618.
81 Y. M. Wang, Z. Y. Wu, H. J. Wang and J. H. Zhu, *Adv. Funct. Mater.*, 2006, **16**, 2374.
82 W. B. Yue and W. Z. Zhou, *J. Mater. Chem.*, 2007, **17**, 4947.
83 H. Yen, Y. Seo, R. Guillet-Nicolas, S. Kaliaguine and F. Kleitz, *Chem. Commun.*, 2011, **47**, 10473.
84 X. Y. Lai, X. T. Li, W. C. Geng, J. C. Tu, J. X. Li and S. L. Qiu, *Angew. Chem., Int. Ed.*, 2007, **46**, 738.
85 J. Roggenbuck, G. Koch and M. Tiemann, *Chem. Mater.*, 2006, **18**, 4151.
86 X. H. Sun, Y. F. Shi, P. Zhang, C. M. Zheng, X. Y. Zheng, F. Zhang, Y. C. Zhang, N. J. Guan, D. Y. Zhao and G. D. Stucky, *J. Am. Chem. Soc.*, 2011, **133**, 14542.
87 Z. X. Wu, Q. Li, D. Peng, P. A. Webley and D. Y. Zhao, *J. Am. Chem. Soc.*, 2010, **132**, 12042.
88 B. Z. Tian, X. Y. Liu, C. Z. Yu, F. Gao, Q. Luo, S. H. Xie, B. Tu and D. Y. Zhao, *Chem. Commun.*, 2002, 1186.
89 D. Gu, F. Q. Zhang, Y. F. Shi, F. Zhang, Z. X. Wu, Y. H. Deng, L. J. Zhang, B. Tu and D. Y. Zhao, *J. Colloid Interface Sci.*, 2008, **328**, 338.
90 H. Tüysüz, E. L. Salabas, E. Bill, H. Bongard, B. Spliethoff, C. W. Lehmann and F. Schüth, *Chem. Mater.*, 2012, **24**, 2493.
91 A. Stein and R. C. Schroden, *Curr. Opin. Solid State Mater. Sci.*, 2001, **5**, 553.
92 O. D. Velev and E. W. Kaler, *Adv. Mater.*, 2000, **12**, 531.
93 H. W. Yan, C. F. Blanford, B. T. Holland, W. H. Smyrl and A. Stein, *Chem. Mater.*, 2000, **12**, 1134.
94 C. F. Blanford, H. W. Yan, R. C. Schroden, M. Al-Daous and A. Stein, *Adv. Mater.*, 2001, **13**, 401.
95 H. W. Yan, C. F. Blanford, B. T. Holland, M. Parent, W. H. Smyrl and A. Stein, *Adv. Mater.*, 1999, **11**, 1003.
96 B. T. Holland, C. F. Blanford and A. Stein, *Science*, 1998, **281**, 538.
97 J. Wijnhoven and W. L. Vos, *Science*, 1998, **281**, 802.
98 B. T. Holland, C. F. Blanford, T. Do and A. Stein, *Chem. Mater.*, 1999, **11**, 795.
99 A. Richel, N. P. Johnson and D. W. McComb, *Appl. Phys. Lett.*, 2000, **76**, 1816.
100 D. W. McComb, B. M. Treble, C. J. Smith, R. M. De La Rue and N. P. Johnson, *J. Mater. Chem.*, 2001, **11**, 142.
101 M. E. Turner, T. J. Trentler and V. L. Colvin, *Adv. Mater.*, 2001, **13**, 180.
102 E. J. W. Crossland, N. Noel, V. Sivaram, T. Leijtens, J. A. Alexander-Webber and H. J. Snaith, *Nature*, 2013, **495**, 215.
103 C. F. Blanford, T. N. Do, B. T. Holland and A. Stein, *Mater. Res. Soc. Symp. Proc.*, 1999, **549**, 61.
104 S. A. Johnson, P. J. Ollivier and T. E. Mallouk, *Science*, 1999, **283**, 963.
105 Z. J. Li and M. Jaroniec, *J. Am. Chem. Soc.*, 2001, **123**, 9208.
106 Z. Y. Yuan and B. L. Su, *J. Mater. Chem.*, 2006, **16**, 663.
107 B. T. Holland, L. Abrams and A. Stein, *J. Am. Chem. Soc.*, 1999, **121**, 4308.
108 G. Gundiah, *Bull. Mater. Sci.*, 2001, **24**, 211.
109 M. Faustini, M. Vayer, B. Marmiroli, M. Hillmyer, H. Amenitsch, C. Sinturel and D. Grosso, *Chem. Mater.*, 2010, **22**, 5687.
110 E. J. W. Crossland, M. Nedelcu, C. Ducati, S. Ludwigs, M. A. Hillmyer, U. Steiner and H. J. Snaith, *Nano Lett.*, 2009, **9**, 2813.

111 M. R. J. Scherer, L. Li, P. M. S. Cunha, O. A. Scherman and U. Steiner, *Adv. Mater.*, 2012, **24**, 1217.
112 A. Corma, P. Atienzar, H. Garcia and J. Y. Chane-Ching, *Nat. Mater.*, 2004, **3**, 394.
113 J. H. Ba, J. Polleux, M. Antonietti and M. Niederberger, *Adv. Mater.*, 2005, **17**, 2509.
114 T. Brezesinski, J. Wang, J. Polleux, B. Dunn and S. H. Tolbert, *J. Am. Chem. Soc.*, 2009, **131**, 1802.
115 R. Buonsanti, T. E. Pick, N. Krins, T. J. Richardson, B. A. Helms and D. J. Milliron, *Nano Lett.*, 2012, **12**, 3872.
116 I. E. Rauda, R. Buonsanti, L. C. Saldarriaga-Lopez, K. Benjauthrit, L. T. Schelhas, M. Stefik, V. Augustyn, J. Ko, B. Dunn, U. Wiesner, D. J. Milliron and S. H. Tolbert, *ACS Nano*, 2012, **6**, 6386.
117 M. Yada, H. Kitamura, A. Ichinose, M. Machida and T. Kijima, *Angew. Chem., Int. Ed.*, 1999, **38**, 3506.
118 D. M. Lyons, L. P. Harman and M. A. Morris, *J. Mater. Chem.*, 2004, **14**, 1976.
119 Q. Yuan, A. X. Yin, C. Luo, L. D. Sun, Y. W. Zhang, W. T. Duan, H. C. Liu and C. H. Yan, *J. Am. Chem. Soc.*, 2008, **130**, 3465.
120 S. Valange, J. L. Guth, F. Kolenda, S. Lacombe and Z. Gabelica, *Microporous Mesoporous Mater.*, 2000, **35–36**, 597.
121 M. Templin, A. Franck, A. DuChesne, H. Leist, Y. M. Zhang, R. Ulrich, V. Schadler and U. Wiesner, *Science*, 1997, **278**, 1795.
122 M. Kuemmel, D. Grosso, U. Boissière, B. Smarsly, T. Brezesinski, P. A. Albouy, H. Amenitsch and C. Sanchez, *Angew. Chem., Int. Ed.*, 2005, **44**, 4589.
123 K. Brezesinski, R. Ostermann, P. Hartmann, J. Perlich and T. Brezesinski, *Chem. Mater.*, 2010, **22**, 3079.
124 Y. Castro, B. Julian, C. Boissière, B. Viana, H. Amenitsch, D. Grosso and C. Sanchez, *Nanotechnology*, 2007, **18**, 055705.
125 T. Brezesinski, M. Groenewolt, M. Antonietti and B. Smarsly, *Angew. Chem., Int. Ed.*, 2006, **45**, 781.
126 T. Brezesinski, B. Smarsly, K. Iimura, D. Grosso, C. Boissière, H. Amenitsch, M. Antonietti and C. Sanchez, *Small*, 2005, **1**, 889.
127 T. Brezesinski, J. Wang, S. H. Tolbert and B. Dunn, *Nat. Mater.*, 2010, **9**, 146.
128 K. Brezesinski, J. Wang, J. Haetge, C. Reitz, S. O. Steinmueller, S. H. Tolbert, B. M. Smarsly, B. Dunn and T. Brezesinski, *J. Am. Chem. Soc.*, 2010, **132**, 6982.
129 T. Brezesinski, A. Fischer, K. I. Iimura, C. Sanchez, D. Grosso, M. Antonietti and B. M. Smarsly, *Adv. Funct. Mater.*, 2006, **16**, 1433.
130 B. Smarsly, D. Grosso, T. Brezesinski, N. Pinna, C. Boissière, M. Antonietti and C. Sanchez, *Chem. Mater.*, 2004, **16**, 2948.
131 T. Brezesinski, D. Fattakhova-Rohlfing, S. Sallard, M. Antonietti and B. M. Smarsly, *Small*, 2006, **2**, 1203.
132 Y. Castro, B. Julian-Lopez, C. Boissière, B. Viana, D. Grosso and C. Sanchez, *Microporous Mesoporous Mater.*, 2007, **103**, 273.
133 J. Lee, M. C. Orilall, S. C. Warren, M. Kamperman, F. J. Disalvo and U. Wiesner, *Nat. Mater.*, 2008, **7**, 222.
134 M. C. Orilall, F. Matsumoto, Q. Zhou, H. Sai, H. D. Abruna, F. J. DiSalvo and U. Wiesner, *J. Am. Chem. Soc.*, 2009, **131**, 9389.
135 C. Sassoye, C. Laberty, H. Le Khanh, S. Cassaignon, C. Boissière, M. Antonietti and C. Sanchez, *Adv. Funct. Mater.*, 2009, **19**, 1922.
136 J. Y. Zhang, Y. H. Deng, D. Gu, S. T. Wang, L. She, R. C. Che, Z. S. Wang, B. Tu, S. H. Xie and D. Y. Zhao, *Adv. Energy Mater.*, 2011, **1**, 241.
137 S. A. Bagshaw and T. J. Pinnavaia, *Angew. Chem., Int. Ed. Engl.*, 1996, **35**, 1102.
138 J. Aguado, J. M. Escola, M. C. Castro and B. Paredes, *Microporous Mesoporous Mater.*, 2005, **83**, 181.
139 M. B. Yue, W. Q. Jiao, Y. M. Wang and M. Y. He, *Microporous Mesoporous Mater.*, 2010, **132**, 226.
140 M. B. Yue, T. Xue, W. Q. Jiao, Y. M. Wang and M. Y. He, *Solid State Sci.*, 2011, **13**, 409.
141 D. N. Srivastava, N. Perkas, A. Gedanken and I. Felner, *J. Phys. Chem. B*, 2002, **106**, 1878.
142 A. S. Malik, M. J. Duncan and P. G. Bruce, *J. Mater. Chem.*, 2003, **13**, 2123.
143 M. Yada, M. Ohya, M. Machida and T. Kijima, *Langmuir*, 2000, **16**, 4752.
144 P. Liu, J. Liu and A. Sayari, *Chem. Commun.*, 1997, 577.
145 W. Xing, F. Li, Z. F. Yan and G. Q. Lu, *J. Power Sources*, 2004, **134**, 324.
146 K. G. Severin, T. M. Abdel-Fattah and T. J. Pinnavaia, *Chem. Commun.*, 1998, 1471.
147 Y. Q. Wang, X. H. Tang, L. X. Yin, W. P. Huang, Y. R. Hacohen and A. Gedanken, *Adv. Mater.*, 2000, **12**, 1183.
148 S. H. Baeck, K. S. Choi, T. F. Jaramillo, G. D. Stucky and E. W. McFarland, *Adv. Mater.*, 2003, **15**, 1269.
149 M. S. Wong and J. Y. Ying, *Chem. Mater.*, 1998, **10**, 2067.
150 O. Dag, I. Soten, O. Celik, S. Polarz, N. Coombs and G. A. Ozin, *Adv. Funct. Mater.*, 2003, **13**, 30.
151 Y. Zhou and M. Antonietti, *J. Am. Chem. Soc.*, 2003, **125**, 14960.
152 L. Malfatti, M. G. Bellino, P. Innocenzi and G. J. A. A. Soler-Illia, *Chem. Mater.*, 2009, **21**, 2763.
153 Y. Q. Wang, C. M. Yang, W. Schmidt, B. Spliethoff, E. Bill and F. Schüth, *Adv. Mater.*, 2005, **17**, 53.
154 F. Jiao, A. H. Hill, A. Harrison, A. Berko, A. V. Chadwick and P. G. Bruce, *J. Am. Chem. Soc.*, 2008, **130**, 5262.
155 H. Tüysüz, M. Comotti and F. Schüth, *Chem. Commun.*, 2008, 4022.
156 H. Tüysüz, C. W. Lehmann, H. Bongard, B. Tesche, R. Schmidt and F. Schüth, *J. Am. Chem. Soc.*, 2008, **130**, 11510.
157 B. Ohtani, Y. Ogawa and S. Nishimoto, *J. Phys. Chem. B*, 1997, **101**, 3746.
158 J. N. Kondo and K. Domen, *Chem. Mater.*, 2008, **20**, 835.
159 T. Katou, B. Lee, D. L. Lu, J. N. Kondo, M. Hara and K. Domen, *Angew. Chem., Int. Ed.*, 2003, **42**, 2382.
160 R. Y. Zhang, B. Tu and D. Y. Zhao, *Chem.–Eur. J.*, 2010, **16**, 9977.

161 H. F. Yang, Q. H. Shi, B. Z. Tian, Q. Y. Lu, F. Gao, S. H. Xie, J. Fan, C. Z. Yu, B. Tu and D. Y. Zhao, *J. Am. Chem. Soc.*, 2003, **125**, 4724.
162 W. B. Yue, A. H. Hill, A. Harrison and W. Z. Zhou, *Chem. Commun.*, 2007, 2518.
163 P. Mohanty, Y. W. Fei and K. Landskron, *J. Am. Chem. Soc.*, 2009, **131**, 9638.
164 P. Mohanty, V. Ortalan, N. D. Browning, I. Arslan, Y. W. Fei and K. Landskron, *Angew. Chem., Int. Ed.*, 2010, **49**, 4301.
165 D. Grosso, F. Ribot, C. Boissière and C. Sanchez, *Chem. Soc. Rev.*, 2011, **40**, 829.
166 K. Niesz, P. D. Yang and G. A. Somorjai, *Chem. Commun.*, 2005, 1986.
167 L. L. Li, W. T. Duan, Q. Yuan, Z. X. Li, H. H. Duan and C. H. Yan, *Chem. Commun.*, 2009, 6174.
168 S. M. Morris, P. F. Fulvio and M. Jaroniec, *J. Am. Chem. Soc.*, 2008, **130**, 15210.
169 S. M. Grant and M. Jaroniec, *J. Mater. Chem.*, 2012, **22**, 86.
170 F. Jiao and P. G. Bruce, *Angew. Chem., Int. Ed.*, 2004, **43**, 5958.
171 Z. R. Tian, W. Tong, J. Y. Wang, N. G. Duan, V. V. Krishnan and S. L. Suib, *Science*, 1997, **276**, 926.
172 D. M. Antonelli and J. Y. Ying, *Angew. Chem., Int. Ed. Engl.*, 1996, **35**, 426.
173 T. Sun and J. Y. Ying, *Nature*, 1997, **389**, 704.
174 X. Xu, B. Z. Tian, J. L. Kong, S. Zhang, B. H. Liu and D. Y. Zhao, *Adv. Mater.*, 2003, **15**, 1932.
175 X. Xu, B. Z. Tian, S. Zhang, J. L. Kong, D. Y. Zhao and B. H. Liu, *Anal. Chim. Acta*, 2004, **519**, 31.
176 S. Banerjee, A. Santhanam, A. Dhathathreyan and P. M. Rao, *Langmuir*, 2003, **19**, 5522.
177 D. D. Zhao, M. W. Xu, W. H. Zhou, J. Zhang and H. L. Li, *Electrochim. Acta*, 2008, **53**, 2699.
178 N. Ulagappan and C. N. R. Rao, *Chem. Commun.*, 1996, 1685.
179 T. Hyodo, N. Nishida, Y. Shimizu and M. Egashira, *Sens. Actuators, B*, 2002, **83**, 209.
180 T. Hyodo, S. Abe, Y. Shimizu and M. Egashira, *Sens. Actuators, B*, 2003, **93**, 590.
181 D. M. Antonelli and J. Y. Ying, *Chem. Mater.*, 1996, **8**, 874.
182 J. J. Kang, Y. X. Rao, M. Trudeau and D. Antonelli, *Angew. Chem., Int. Ed.*, 2008, **47**, 4896.
183 S. H. Zhan, D. R. Chen, X. L. Jiao and C. H. Tao, *J. Phys. Chem. B*, 2006, **110**, 11199.
184 W. Y. Dong, Y. J. Sun, C. W. Lee, W. M. Hua, X. C. Lu, Y. F. Shi, S. C. Zhang, J. M. Chen and D. Y. Zhao, *J. Am. Chem. Soc.*, 2007, **129**, 13894.
185 R. L. Liu, Y. J. Ren, Y. F. Shi, F. Zhang, L. J. Zhang, B. Tu and D. Y. Zhao, *Chem. Mater.*, 2008, **20**, 1140.
186 C. H. Huang, D. Gu, D. Y. Zhao and R. A. Doong, *Chem. Mater.*, 2010, **22**, 1760.
187 A. Mitra, D. Jana and G. De, *Chem. Commun.*, 2012, **48**, 3333.
188 A. K. Sinha and K. Suzuki, *Angew. Chem., Int. Ed.*, 2005, **44**, 271.
189 E. Ortel, A. Fischer, L. Chuenchom, J. Polte, F. Emmerling, B. Smarsly and R. Kraehnert, *Small*, 2012, **8**, 298.
190 B. Lee, D. L. Lu, J. N. Kondo and K. Domen, *J. Am. Chem. Soc.*, 2002, **124**, 11256.
191 C. W. Wu, T. Ohsuna, M. Kuwabara and K. Kuroda, *J. Am. Chem. Soc.*, 2006, **128**, 4544.
192 S. Y. Choi, B. Lee, D. B. Carew, M. Mamak, F. C. Peiris, S. Speakman, N. Chopra and G. A. Ozin, *Adv. Funct. Mater.*, 2006, **16**, 1731.
193 J. L. Chen, C. Burger, C. V. Krishnan and B. Chu, *J. Am. Chem. Soc.*, 2005, **127**, 14140.
194 J. Cejka, *Appl. Catal., A*, 2003, **254**, 327.
195 Q. S. Huo, D. I. Margolese, U. Ciesla, D. G. Demuth, P. Y. Feng, T. E. Gier, P. Sieger, A. Firouzi, B. F. Chmelka, F. Schüth and G. D. Stucky, *Chem. Mater.*, 1994, **6**, 1176.
196 U. Ciesla, D. Demuth, R. Leon, P. Petroff, G. D. Stucky, K. Unger and F. Schüth, *J. Chem. Soc., Chem. Commun.*, 1994, 1387.
197 F. Vaudry, S. Khodabandeh and M. E. Davis, *Chem. Mater.*, 1996, **8**, 1451.
198 M. Yada, M. Machida and T. Kijima, *Chem. Commun.*, 1996, 769.
199 Z. R. Zhang and T. J. Pinnavaia, *J. Am. Chem. Soc.*, 2002, **124**, 12294.
200 Z. R. Zhang, R. W. Hicks, T. R. Pauly and T. J. Pinnavaia, *J. Am. Chem. Soc.*, 2002, **124**, 1592.
201 B. Z. Tian, H. F. Yang, X. Y. Liu, S. H. Xie, C. Z. Yu, J. Fan, B. Tu and D. Y. Zhao, *Chem. Commun.*, 2002, 1824.
202 W. C. Li, A. H. Lu, W. Schmidt and F. Schüth, *Chem.–Eur. J.*, 2005, **11**, 1658.
203 Q. Liu, A. Q. Wang, X. D. Wang and T. Zhang, *Chem. Mater.*, 2006, **18**, 5153.
204 W. Li, Y. H. Deng, Z. X. Wu, X. F. Qian, J. P. Yang, Y. Wang, D. Gu, F. Zhang, B. Tu and D. Y. Zhao, *J. Am. Chem. Soc.*, 2011, **133**, 15830.
205 T. Fröschl, U. Hörmann, P. Kubiak, G. Kučerová, M. Pfanzelt, C. K. Weiss, R. J. Behm, N. Hüsing, U. Kaiser, K. Landfester and M. Wohlfahrt-Mehrens, *Chem. Soc. Rev.*, 2012, **41**, 5313.
206 S. Guldin, P. Docampo, M. Stefik, G. Kamita, U. Wiesner, H. J. Snaith and U. Steiner, *Small*, 2012, **8**, 432.
207 J. T. Park, W. S. Chi, D. K. Roh, S. H. Ahn and J. H. Kim, *Adv. Funct. Mater.*, 2013, **23**, 26.
208 G. Soler-Illia, P. C. Angelome, M. C. Fuertes, D. Grosso and C. Boissière, *Nanoscale*, 2012, **4**, 2549.
209 M. Thieme and F. Schüth, *Microporous Mesoporous Mater.*, 1999, **27**, 193.
210 D. M. Antonelli, *Microporous Mesoporous Mater.*, 1999, **30**, 315.
211 P. C. A. Alberius, K. L. Frindell, R. C. Hayward, E. J. Kramer, G. D. Stucky and B. F. Chmelka, *Chem. Mater.*, 2002, **14**, 3284.
212 M. Faustini, B. Louis, P. A. Albouy, M. Kuemmel and D. Grosso, *J. Phys. Chem. C*, 2010, **114**, 7637.
213 N. Krins, M. Faustini, B. Louis and D. Grosso, *Chem. Mater.*, 2010, **22**, 6218.
214 D. Grosso, G. Illia, E. L. Crepaldi, B. Charleux and C. Sanchez, *Adv. Funct. Mater.*, 2003, **13**, 37.

215 S. Y. Choi, M. Mamak, N. Coombs, N. Chopra and G. A. Ozin, *Adv. Funct. Mater.*, 2004, **14**, 335.
216 H. Choi, A. C. Sofranko and D. D. Dionysiou, *Adv. Funct. Mater.*, 2006, **16**, 1067.
217 H. Shibata, T. Ogura, T. Mukai, T. Ohkubo, H. Sakai and M. Abe, *J. Am. Chem. Soc.*, 2005, **127**, 16396.
218 H. Shibata, H. Mihara, T. Mlikai, T. Ogura, H. Kohno, T. Ohkubo, H. Sakait and M. Abe, *Chem. Mater.*, 2006, **18**, 2256.
219 S. S. Kim, H. I. Lee, J. K. Shon, J. Y. Hur, M. S. Kang, S. S. Park, S. S. Kong, J. A. Yu, M. Seo, D. Li, S. S. Thakur and J. M. Kim, *Chem. Lett.*, 2008, 140.
220 W. B. Yue, C. Randorn, P. S. Attidekou, Z. X. Su, J. T. S. Irvine and W. Z. Zhou, *Adv. Funct. Mater.*, 2009, **19**, 2826.
221 W. B. Yue, X. X. Xu, J. T. S. Irvine, P. S. Attidekou, C. Liu, H. Y. He, D. Y. Zhao and W. Z. Zhou, *Chem. Mater.*, 2009, **21**, 2540.
222 Y. Ren, L. J. Hardwick and P. G. Bruce, *Angew. Chem., Int. Ed.*, 2010, **49**, 2570.
223 T. Yamaguchi, *Catal. Today*, 1994, **20**, 199.
224 J. Kaspar, P. Fornasiero and N. Hickey, *Catal. Today*, 2003, **77**, 419.
225 Y. Nakano, T. Iizuka, H. Hattori and K. Tanabe, *J. Catal.*, 1979, **57**, 1.
226 X. Yang, F. C. Jentoft, R. E. Jentoft, F. Girgsdies and T. Ressler, *Catal. Lett.*, 2002, **81**, 25.
227 U. Ciesla, S. Schacht, G. D. Stucky, K. K. Unger and F. Schüth, *Angew. Chem., Int. Ed. Engl.*, 1996, **35**, 541.
228 U. Ciesla, M. Froba, G. D. Stucky and F. Schüth, *Chem. Mater.*, 1999, **11**, 227.
229 J. A. Knowles and M. J. Hudson, *J. Chem. Soc., Chem. Commun.*, 1995, 2083.
230 M. J. Hudson and J. A. Knowles, *J. Mater. Chem.*, 1996, **6**, 89.
231 D. Khushalani, O. Dag, G. A. Ozin and A. Kuperman, *J. Mater. Chem.*, 1999, **9**, 1491.
232 S. Y. Chen, L. Y. Jang and S. Cheng, *J. Phys. Chem. B*, 2006, **110**, 11761.
233 B. Liu and R. T. Baker, *J. Mater. Chem.*, 2008, **18**, 5200.
234 Z. F. Li and E. Ruckenstein, *Langmuir*, 2002, **18**, 6956.
235 V. Luca, D. J. MacLachlan, J. M. Hook and R. Withers, *Chem. Mater.*, 1995, **7**, 2220.
236 V. Luca and J. M. Hook, *Chem. Mater.*, 1997, **9**, 2731.
237 P. Liu, I. L. Moudrakovski, J. Liu and A. Sayari, *Chem. Mater.*, 1997, **9**, 2513.
238 D. M. Antonelli, A. Nakahira and J. Y. Ying, *Inorg. Chem.*, 1996, **35**, 3126.
239 D. M. Antonelli, *Microporous Mesoporous Mater.*, 1999, **33**, 209.
240 X. Y. Chen, T. Yu, X. X. Fan, H. T. Zhang, Z. S. Li, J. h. Ye and Z. G. Zou, *Appl. Surf. Sci.*, 2007, **253**, 8500.
241 L. Ye, S. H. Xie, B. Yue, L. P. Qian, S. J. Feng, S. C. Tsang, Y. C. Li and H. Y. He, *CrystEngComm*, 2010, **12**, 344.
242 S. Seki, T. Unagami and O. Kogure, *J. Electrochem. Soc.*, 1985, **132**, 3054.
243 Y. Takahara, J. N. Kondo, T. Takata, D. L. Lu and K. Domen, *Chem. Mater.*, 2001, **13**, 1194.
244 N. R. Jana, Y. F. Chen and X. G. Peng, *Chem. Mater.*, 2004, **16**, 3931.
245 T. Yokoyama and N. Fujita, *Appl. Catal., A*, 2004, **276**, 179.
246 H. Tüysüz, C. Weidenthaler, T. Grewe, E. L. Salabas, M. J. B. Romero and F. Schüth, *Inorg. Chem.*, 2012, **51**, 11745.
247 L. Dupont, S. Laruelle, S. Grugeon, C. Dickinson, W. Zhou and J. M. Tarascon, *J. Power Sources*, 2008, **175**, 502.
248 H. Liu, X. W. Du, X. R. Xing, G. X. Wang and S. Z. Qiao, *Chem. Commun.*, 2012, **48**, 865.
249 Y. Xia, H. Dai, H. Jiang, J. Deng, H. He and C. T. Au, *Environ. Sci. Technol.*, 2009, **43**, 8355.
250 I. Tamiolakis, I. N. Lykakis, A. P. Katsoulidis, C. D. Malliakas and G. S. Armatas, *J. Mater. Chem.*, 2012, **22**, 6919.
251 Y. Liu, Y. Qian, M. Zhang, Z. Chen and C. Wang, *Mater. Res. Bull.*, 1996, **31**, 1029.
252 H. C. Zeng, *Inorg. Chem.*, 1998, **37**, 1967.
253 Z. Hussain, *J. Mater. Res.*, 2001, **16**, 2695.
254 J. N. Yao, K. Hashimoto and A. Fujishima, *Nature*, 1992, **355**, 624.
255 D. M. Antonelli and M. Trudeau, *Angew. Chem., Int. Ed.*, 1999, **38**, 1471.
256 M. S. Whittingham, J. D. Guo, R. J. Chen, T. Chirayil, G. Janauer and P. Zavalij, *Solid State Ionics*, 1995, **75**, 257.
257 G. G. Janauer, A. Dobley, J. D. Guo, P. Zavalij and M. S. Whittingham, *Chem. Mater.*, 1996, **8**, 2096.
258 M. Niederberger, F. Krumeich, H. J. Muhr, M. Muller and R. Nesper, *J. Mater. Chem.*, 2001, **11**, 1941.
259 R. Q. Song, A. W. Xu, B. Deng and Y. P. Fang, *J. Phys. Chem. B*, 2005, **109**, 22758.
260 X. J. Yu, Z. H. Xu, S. H. Han, H. W. Che, X. Yan and A. F. Liu, *Colloids Surf., A*, 2009, **333**, 194.
261 X. J. Yu, Z. H. Xu and S. H. Han, *J. Porous Mater.*, 2010, **17**, 99.
262 C. Santato, M. Odziemkowski, M. Ulmann and J. Augustynski, *J. Am. Chem. Soc.*, 2001, **123**, 10639.
263 S. Pokhrel, C. E. Simion, V. S. Teodorescu, N. Barsan and U. Weimar, *Adv. Funct. Mater.*, 2009, **19**, 1767.
264 E. Rossinyol, J. Arbiol, F. Peiro, A. Cornet, J. R. Morante, B. Z. Tian, T. Bo and D. Y. Zhao, *Sens. Actuators, B*, 2005, **109**, 57.
265 E. Rossinyol, A. Prim, E. Pellicer, J. Arbiol, F. Hernandez-Ramirez, F. Peiro, A. Cornet, J. R. Morante, L. A. Solovyov, B. Z. Tian, T. Bo and D. Y. Zhao, *Adv. Funct. Mater.*, 2007, **17**, 1801.
266 L. Zhou, Q. J. Ren, X. F. Zhou, J. W. Tang, Z. H. Chen and C. Z. Yu, *Microporous Mesoporous Mater.*, 2008, **109**, 248.
267 E. Kang, S. An, S. Yoon, J. K. Kim and J. Lee, *J. Mater. Chem.*, 2010, **20**, 7416.
268 S. Yoon, E. Kang, J. K. Kim, C. W. Lee and J. Lee, *Chem. Commun.*, 2011, **47**, 1021.
269 C. Jo, I. Hwang, J. Lee, C. W. Lee and S. Yoon, *J. Phys. Chem. C*, 2011, **115**, 11880.

270 A. K. Sinha, K. Suzuki, M. Takahara, H. Azuma, T. Nonaka and K. Fukumoto, *Angew. Chem., Int. Ed.*, 2007, **46**, 2891.
271 J. Y. Luo, J. J. Zhang and Y. Y. Xia, *Chem. Mater.*, 2006, **18**, 5618.
272 F. Jiao and P. G. Bruce, *Adv. Mater.*, 2007, **19**, 657.
273 Y. Ren, A. R. Armstrong, F. Jiao and P. G. Bruce, *J. Am. Chem. Soc.*, 2010, **132**, 996.
274 H. R. Chen, X. P. Dong, J. L. Shi, J. J. Zhao, Z. L. Hua, J. H. Gao, M. L. Ruan and D. S. Yan, *J. Mater. Chem.*, 2007, **17**, 855.
275 R. A. Chandru, S. Patra, C. Oommen, N. Munichandraiah and B. N. Raghunandan, *J. Mater. Chem.*, 2012, **22**, 6536.
276 K. Brezesinski, J. Haetge, J. Wang, S. Mascotto, C. Reitz, A. Rein, S. H. Tolbert, J. Perlich, B. Dunn and T. Brezesinski, *Small*, 2011, **7**, 407.
277 P. Wang and I. M. C. Lo, *Water Res.*, 2009, **43**, 3727.
278 F. Jiao, J. C. Jumas, M. Womes, A. V. Chadwick, A. Harrison and P. G. Bruce, *J. Am. Chem. Soc.*, 2006, **128**, 12905.
279 E. Delahaye, V. Escax, N. El Hassan, A. Davidson, R. Aquino, V. Dupuis, R. Perzynski and Y. L. Raikher, *J. Phys. Chem. B*, 2006, **110**, 26001.
280 T. A. Crowley, K. J. Ziegler, D. M. Lyons, D. Erts, H. Olin, M. A. Morris and J. D. Holmes, *Chem. Mater.*, 2003, **15**, 3518.
281 H. Tüysüz, E. L. Salabas, C. Weidenthaler and F. Schüth, *J. Am. Chem. Soc.*, 2008, **130**, 280.
282 H. Tüysüz, C. Weidenthaler and F. Schüth, *Chem.–Eur. J.*, 2012, **18**, 5080.
283 P. Poizot, S. Laruelle, S. Grugeon, L. Dupont and J. M. Tarascon, *Nature*, 2000, **407**, 496.
284 W. Y. Li, L. N. Xu and J. Chen, *Adv. Funct. Mater.*, 2005, **15**, 851.
285 T. Maruyama and S. Arai, *J. Electrochem. Soc.*, 1996, **143**, 1383.
286 C. Dickinson, W. Z. Zhou, R. P. Hodgkins, Y. F. Shi, D. Y. Zhao and H. Y. He, *Chem. Mater.*, 2006, **18**, 3088.
287 A. Rumplecker, F. Kleitz, E. L. Salabas and F. Schüth, *Chem. Mater.*, 2007, **19**, 485.
288 K. M. Shaju, F. Jiao, A. Débart and P. G. Bruce, *Phys. Chem. Chem. Phys.*, 2007, **9**, 1837.
289 Y. G. Wang, Y. Q. Wang, J. W. Ren, Y. Mi, F. Y. Zhang, C. L. Li, X. H. Liu, Y. Guo, Y. L. Guo and G. Z. Lu, *J. Solid State Chem.*, 2010, **183**, 277.
290 H. X. Jin, X. J. Gu, B. Hong, L. S. Lin, C. Y. Wang, D. F. Jin, X. L. Peng, X. Q. Wang and H. L. Ge, *J. Phys. Chem. C*, 2012, **116**, 13374.
291 H. Tüysüz, Y. Liu, C. Weidenthaler and F. Schüth, *J. Am. Chem. Soc.*, 2008, **130**, 14108.
292 Y. Ren, Z. Ma, L. P. Qian, S. Dai, H. Y. He and P. G. Bruce, *Catal. Lett.*, 2009, **131**, 146.
293 M. J. Benitez, O. Petracic, E. L. Salabas, F. Radu, H. Tüysüz, F. Schüth and H. Zabel, *Phys. Rev. Lett.*, 2008, **101**, 097206.
294 M. J. Benitez, O. Petracic, H. Tüysüz, F. Schüth and H. Zabel, *EPL*, 2009, **88**, 27004.
295 M. J. Benitez, O. Petracic, H. Tüysüz, F. Schüth and H. Zabel, *Phys. Rev. B: Condens. Matter Mater. Phys.*, 2011, **83**, 134424.
296 N. Dahal, I. A. Ibarra and S. M. Humphrey, *J. Mater. Chem.*, 2012, **22**, 12675.
297 Y. G. Wang and Y. Y. Xia, *Electrochim. Acta*, 2006, **51**, 3223.
298 V. Subramanian, S. C. Hall, P. H. Smith and B. Rambabu, *Solid State Ionics*, 2004, **175**, 511.
299 J. N. Park, J. K. Shon, M. Jin, S. S. Kong, K. Moon, G. O. Park, J. H. Boo and J. M. Kim, *React. Kinet., Mech. Catal.*, 2011, **103**, 87.
300 M. Matsuoka, W. S. Ju, K. Takahashi, H. Yamashita and M. Anpo, *J. Phys. Chem. B*, 2000, **104**, 4911.
301 A. Martinez-Arias, M. Fernandez-Garcia, O. Galvez, J. M. Coronado, J. A. Anderson, J. C. Conesa, J. Soria and G. Munuera, *J. Catal.*, 2000, **195**, 207.
302 J. B. Reitz and E. I. Solomon, *J. Am. Chem. Soc.*, 1998, **120**, 11467.
303 H. M. Luo, J. F. Zhang and Y. S. Yan, *Chem. Mater.*, 2003, **15**, 3769.
304 Y. Shang, D. F. Zhang and L. Guo, *J. Mater. Chem.*, 2012, **22**, 856.
305 T. Pauporte and J. Rathousky, *J. Phys. Chem. C*, 2007, **111**, 7639.
306 D. Chandra, S. Mridha, D. Basak and A. Bhaumik, *Chem. Commun.*, 2009, 2384.
307 S. Polarz, A. V. Orlov, F. Schüth and A. H. Lu, *Chem.–Eur. J.*, 2007, **13**, 592.
308 T. Waitz, M. Tiemann, P. J. Klar, J. Sann, J. Stehr and B. K. Meyer, *Appl. Phys. Lett.*, 2007, **90**, 123108.
309 T. Wagner, T. Waitz, J. Roggenbuck, M. Froba, C. D. Kohl and M. Tiemann, *Thin Solid Films*, 2007, **515**, 8360.
310 A. Chernikov, S. Horst, T. Waitz, M. Tiemann and S. Chatterjee, *J. Phys. Chem. C*, 2011, **115**, 1375.
311 S. Lepoutre, B. Julian-Lopez, C. Sanchez, H. Amenitsch, M. Linden and D. Grosso, *J. Mater. Chem.*, 2010, **20**, 537.
312 M. Yada, H. Kitamura, M. Machida and T. Kijima, *Inorg. Chem.*, 1998, **37**, 6470.
313 M. Lundberg, B. Skarman, F. Cesar and L. R. Wallenberg, *Microporous Mesoporous Mater.*, 2002, **54**, 97.
314 J. Hierso, O. Sel, A. Ringuede, C. Laberty-Robert, L. Bianchi, D. Grosso and C. Sanchez, *Chem. Mater.*, 2009, **21**, 2184.
315 G. Mueller, C. Boissière, D. Grosso, A. Ringuede, C. Laberty-Robert and C. Sanchez, *J. Mater. Chem.*, 2012, **22**, 9368.
316 G. Baldinozzi, G. Muller, C. Laberty-Robert, D. Gosset, D. Simeone and C. Sanchez, *J. Phys. Chem. C*, 2012, **116**, 7658.
317 S. C. Laha and R. Ryoo, *Chem. Commun.*, 2003, 2138.
318 W. H. Shen, X. P. Dong, Y. F. Zhu, H. R. Chen and J. L. Shi, *Microporous Mesoporous Mater.*, 2005, **85**, 157.
319 J. Roggenbuck, H. Schaefer, T. Tsoncheva, C. Minchev, J. Hanss and M. Tiemann, *Microporous Mesoporous Mater.*, 2007, **101**, 335.
320 T. K. Kim, K. J. Lee, J. Y. Cheon, J. H. Lee, S. H. Joo and H. R. Moon, *J. Am. Chem. Soc.*, 2013, **135**, 8940.
321 C. J. Jia, Y. Liu, H. Bongard and F. Schüth, *J. Am. Chem. Soc.*, 2010, **132**, 1520.

322 C. X. Liu, L. Zhang, J. G. Deng, Q. Mu, H. X. Dai and H. He, *J. Phys. Chem. C*, 2008, **112**, 19248.
323 H. N. Li, L. Zhang, H. X. Dai and H. He, *Inorg. Chem.*, 2009, **48**, 4421.
324 B. Eckhardt, E. Ortel, J. Polte, D. Bernsmeier, O. Gorke, P. Strasser and R. Kraehnert, *Adv. Mater.*, 2012, **24**, 3115.
325 W. C. Li, A. H. Lu, C. Weidenthaler and F. Schüth, *Chem. Mater.*, 2004, **16**, 5676.
326 J. X. Li, W. L. Dai and K. N. Fan, *J. Phys. Chem. C*, 2008, **112**, 17657.
327 E. Kang, J. Park, Y. Hwang, M. Kang, J. G. Park and T. Hyeon, *J. Phys. Chem. B*, 2004, **108**, 13932.
328 E. Manova, B. Kunev, D. Paneva, I. Mitov, L. Petrov, C. Estournes, C. D'Orleans, J. L. Rehspringer and M. Kurmoo, *Chem. Mater.*, 2004, **16**, 5689.
329 W. F. Wei, W. X. Chen and D. G. Ivey, *Chem. Mater.*, 2008, **20**, 1941.
330 D. Grosso, C. Boissière, B. Smarsly, T. Brezesinski, N. Pinna, P. A. Albouy, H. Amenitsch, M. Antonietti and C. Sanchez, *Nat. Mater.*, 2004, **3**, 787.
331 G. Fortunato, H. R. Oswald and A. Reller, *J. Mater. Chem.*, 2001, **11**, 905.
332 M. A. Carreon, V. V. Guliants, L. Yuan, A. R. Hughett, A. Dozier, G. A. Seisenbaeva and V. G. Kessler, *Eur. J. Inorg. Chem.*, 2006, 4983.
333 X. Q. Tian, L. J. Wan, K. Pan, C. G. Tian, H. G. Fu and K. Y. Shi, *J. Alloys Compd.*, 2009, **488**, 320.
334 W. C. Li, M. Comotti, A. H. Lu and F. Schüth, *Chem. Commun.*, 2006, 1772.
335 T. Valdés-Solís, G. Marbán and A. B. Fuertes, *Chem. Mater.*, 2005, **17**, 1919.
336 F. Jiao, J. l. Bao, A. H. Hill and P. G. Bruce, *Angew. Chem., Int. Ed.*, 2008, **47**, 9711.
337 M. Gu, B. Yue, R. L. Bao and H. Y. He, *Mater. Res. Bull.*, 2009, **44**, 1422.
338 J. K. Zhu and Q. M. Gao, *Microporous Mesoporous Mater.*, 2009, **124**, 144.
339 Y. Y. Sun, G. B. Ji, M. B. Zheng, X. F. Chang, S. D. Li and Y. Zhang, *J. Mater. Chem.*, 2010, **20**, 945.
340 X. Gu, W. M. Zhu, C. J. Jia, R. Zhao, W. Schmidt and Y. Q. Wang, *Chem. Commun.*, 2011, **47**, 5337.
341 T. E. Quickel, V. H. Le, T. Brezesinski and S. H. Tolbert, *Nano Lett.*, 2010, **10**, 2982.
342 J. Y. Luo, Y. G. Wang, H. M. Xiong and Y. Y. Xia, *Chem. Mater.*, 2007, **19**, 4791.
343 C. A. Deshmane, J. B. Jasinski and M. A. Carreon, *Eur. J. Inorg. Chem.*, 2009, 3275.
344 C. A. Deshmane, J. B. Jasinski and M. A. Carreon, *Microporous Mesoporous Mater.*, 2010, **130**, 97.
345 H. F. Yang, Q. Y. Lu, F. Gao, Q. H. Shi, Y. Yan, F. Q. Zhang, S. H. Xie, B. Tu and D. Y. Zhao, *Adv. Funct. Mater.*, 2005, **15**, 1377.
346 T. Waitz, T. Wagner, T. Sauerwald, C. D. Kohl and M. Tiemann, *Adv. Funct. Mater.*, 2009, **19**, 653.
347 X. Y. Lai, D. Wang, N. Han, J. Du, J. Li, C. J. Xing, Y. F. Chen and X. T. Li, *Chem. Mater.*, 2010, **22**, 3033.
348 X. Y. Lai, H. Wang, D. Mao, N. L. Yang, J. X. Yao, C. J. Xing, D. Wang and X. T. Li, *Mater. Lett.*, 2008, **62**, 3868.
349 Q. Y. Lu, F. Gao, Y. Q. Li, Y. M. Zhou and D. Y. Zhao, *Microporous Mesoporous Mater.*, 2002, **56**, 219.
350 X. Chen, Q. Cai, W. Wang, G. Mo, L. S. Jiang, K. H. Zhang, Z. J. Chen, Z. Y. Wu and Z. H. Wu, *J. Phys. Chem. B*, 2008, **112**, 12297.
351 X. D. Zou, T. Conradsson, M. Klingstedt, M. S. Dadachov and M. O'Keeffe, *Nature*, 2005, **437**, 716.
352 C. Aprile, L. Teruel, M. Alvaro and H. Garcia, *J. Am. Chem. Soc.*, 2009, **131**, 1342.
353 H. Kim and J. Cho, *J. Mater. Chem.*, 2008, **18**, 771.
354 T. Wagner, C. D. Kohl, M. Froba and M. Tiemann, *Sensors*, 2006, **6**, 318.
355 B. Hou, Z. J. Li, Y. Xu, D. Wu and Y. H. Sun, *Stud. Surf. Sci. Catal.*, 2005, **156**, 465.
356 Y. G. Wang, J. W. Ren, Y. Q. Wang, F. Y. Zhang, X. H. Liu, Y. Guo and G. Z. Lu, *J. Phys. Chem. C*, 2008, **112**, 15293.
357 R. K. C. de Lima, M. S. Batista, M. Wallau, E. A. Sanches, Y. P. Mascarenhas and E. A. Urquieta-González, *Appl. Catal., B*, 2009, **90**, 441.
358 S. C. Yan, S. X. Ouyang, J. Gao, M. Yang, J. Y. Feng, X. X. Fan, L. J. Wan, Z. S. Li, J. H. Ye, Y. Zhou and Z. G. Zou, *Angew. Chem., Int. Ed.*, 2010, **49**, 6400.
359 X. X. Fan, Y. Wang, X. Y. Chen, L. Gao, W. J. Luo, Y. P. Yuan, Z. S. Li, T. Yu, J. H. Zhu and Z. G. Zou, *Chem. Mater.*, 2010, **22**, 1276.
360 N. Pal, M. Paul and A. Bhaumik, *Appl. Catal., A*, 2011, **393**, 153.
361 X. H. Huang. and M. Li, *Adv. Mater. Res.*, 2011, **306–307**, 1342.
362 M. Faustini, G. L. Drisko, A. A. Letailleur, R. S. Montiel, C. Boissière, A. Cattoni, A. M. Haghiri-Gosnet, G. Lerondel and D. Grosso, *Nanoscale*, 2013, **5**, 984.
363 M. Yada, H. Hiyoshi, K. Ohe, M. Machida and T. Kijima, *Inorg. Chem.*, 1997, **36**, 5565.
364 X. F. Jiang, N. Suzuki, B. P. Bastakoti, K. C. W. Wu and Y. Yamauchi, *Chem.–Asian. J.*, 2012, **7**, 1713.
365 M. Lundberg, B. Skarman and L. R. Wallenberg, *Microporous Mesoporous Mater.*, 2004, **69**, 187.
366 H. Zhang, H. X. Dai, Y. X. Liu, J. G. Deng, L. Zhang and K. M. Ji, *Mater. Chem. Phys.*, 2011, **129**, 586.
367 E. Ortel, T. Reier, P. Strasser and R. Kraehnert, *Chem. Mater.*, 2011, **23**, 3201.
368 J. M. Cao, H. M. Ji, J. S. Liu, M. B. Zheng, X. Chang, X. J. Ma, A. M. Zhang and Q. H. Xu, *Mater. Lett.*, 2005, **59**, 408.
369 P. A. Nelson, J. M. Elliott, G. S. Attard and J. R. Owen, *Chem. Mater.*, 2002, **14**, 524.
370 Y. W. Tan, S. Srinivasan and K. S. Choi, *J. Am. Chem. Soc.*, 2005, **127**, 3596.
371 K. M. Lin, K. H. Chang, C. C. Hu and Y. Y. Li, *Electrochim. Acta*, 2009, **54**, 4574.
372 K. H. Kim, K. S. Kim, G. P. Kim and S. H. Baeck, *Curr. Appl. Phys.*, 2012, **12**, 36.
373 S. Makino, Y. Yamauchi and W. Sugimoto, *J. Power Sources*, 2013, **227**, 153.

374 L. M. Qi, J. M. Ma, H. M. Cheng and Z. G. Zhao, *Langmuir*, 1998, **14**, 2579.
375 F. L. Chen and M. L. Liu, *Chem. Commun.*, 1999, 1829.
376 H. Miyata, M. Itoh, M. Watanabe and T. Noma, *Chem. Mater.*, 2003, **15**, 1334.
377 N. L. Wu and C. Y. Tung, *J. Am. Ceram. Soc.*, 2004, **87**, 1741.
378 Y. H. Yue and Z. Gao, *Chem. Commun.*, 2000, 1755.
379 S. Cabrera, J. El Haskouri, A. Beltran-Porter, D. Beltran-Porter, M. D. Marcos and P. Amoros, *Solid State Sci.*, 2000, **2**, 513.
380 H. S. Yun, K. Miyazawa, H. S. Zhou, I. Honma and M. Kuwabara, *Adv. Mater.*, 2001, **13**, 1377.
381 J. C. Yu, L. Z. Zhang and J. G. Yu, *Chem. Mater.*, 2002, **14**, 4647.
382 H. Yoshitake, T. Sugihara and T. Tatsumi, *Chem. Mater.*, 2002, **14**, 1023.
383 X. C. Wang, J. C. Yu, Y. D. Hou and X. Z. Fu, *Adv. Mater.*, 2005, **17**, 99.
384 V. Luca, J. N. Watson, M. Ruschena and R. B. Knott, *Chem. Mater.*, 2006, **18**, 1156.
385 Y. Zhang, J. Li and J. Wang, *Chem. Mater.*, 2006, **18**, 2917.
386 C. W. Koh, U. H. Lee, J. K. Song, H. R. Lee, M. H. Kim, M. Suh and Y. U. Kwon, *Chem.–Asian. J.*, 2008, **3**, 862.
387 W. Weng, T. Higuchi, M. Suzuki, T. Fukuoka, T. Shimomura, M. Ono, L. Radhakrishnan, H. Wang, N. Suzuki, H. Oveisi and Y. Yamauchi, *Angew. Chem., Int. Ed.*, 2010, **49**, 3956.
388 H. Oveisi, S. Rahighi, X. F. Jiang, Y. Nemoto, A. Beitollahi, S. Wakatsuki and Y. Yamauchi, *Chem.–Asian. J.*, 2010, **5**, 1978.
389 Z. X. Li, F. B. Shi, T. Zhang, H. S. Wu, L. D. Sun and C. H. Yan, *Chem. Commun.*, 2011, **47**, 8109.
390 L. Robben, A. A. Ismail, S. J. Lohmeier, A. Feldhoff, D. W. Bahnemann and J. C. Buhl, *Chem. Mater.*, 2012, **24**, 1268.
391 K. Zimny, T. Rogues-Cannes, C. Carteret, M. J. Stebe and J. L. Blin, *J. Phys. Chem. C*, 2012, **116**, 6585.
392 P. Docampo, M. Stefik, S. Guldin, R. Gunning, N. A. Yufa, N. Cai, P. Wang, U. Steiner, U. Wiesner and H. J. Snaith, *Adv. Energy Mater.*, 2012, **2**, 676.
393 P. Liu, S. H. Lee, C. E. Tracy, Y. F. Yan and J. A. Turner, *Adv. Mater.*, 2002, **14**, 27.
394 W. Cheng, E. Baudrin, B. Dunn and J. I. Zink, *J. Mater. Chem.*, 2001, **11**, 92.
395 J. G. Yuan, Y. Z. Zhang, J. Le, L. X. Song and X. F. Hu, *Mater. Lett.*, 2007, **61**, 1114.
396 A. Y. Ku, W. J. Heward and V. Mani, *J. Mater. Sci.*, 2006, **41**, 3017.
397 V. I. Parvulescu, H. Bonnemann, V. Parvulescu, U. Endruschat, A. Rufinska, C. W. Lehmann, B. Tesche and G. Poncelet, *Appl. Catal., A*, 2001, **214**, 273.
398 A. Vantomme, Z. Y. Yuan and B. L. Su, *New J. Chem.*, 2004, **28**, 1083.
399 G. S. Armatas, G. Bilis and M. Louloudi, *J. Mater. Chem.*, 2011, **21**, 2997.
400 A. Miko, A. L. Demirel and M. Somer, *J. Mater. Chem.*, 2012, **22**, 3705.
401 S. Haffer, C. Weinberger and M. Tiemann, *Eur. J. Inorg. Chem.*, 2012, 3283.
402 Y. G. Wang, X. H. Yuan, X. H. Liu, J. W. Ren, W. Y. Tong, Y. Q. Wang and G. Z. Lu, *Solid State Sci.*, 2008, **10**, 1117.
403 C. West and R. Mokaya, *Chem. Mater.*, 2009, **21**, 4080.
404 M. Imperor-Clerc, D. Bazin, M. D. Appay, P. Beaunier and A. Davidson, *Chem. Mater.*, 2004, **16**, 1813.
405 F. Jiao, A. Harrison, A. H. Hill and P. G. Bruce, *Adv. Mater.*, 2007, **19**, 4063.
406 Z. Y. Zhang, F. Zuo and P. Y. Feng, *J. Mater. Chem.*, 2010, **20**, 2206.
407 K. E. Shopsowitz, A. Stahl, W. Y. Hamad and M. J. MacLachlan, *Angew. Chem., Int. Ed.*, 2012, **51**, 6886.

